

Impact of Continuum Models On Longwave Radiation Fluxes

Mayuri Tatiya
2014

Master of Science (120 credits)
Space Engineering - Space Master

Luleå University of Technology
Department of Computer Science, Electrical and Space Engineering

Impact of Continuum Models On Longwave Radiation Fluxes

Mayuri Tatiya

6 October 2014

CONTENTS

TABLE OF CONTENTS	iii
CHAPTER 1 – INTRODUCTION	3
CHAPTER 2 – BACKGROUND	5
2.1 Radiative transfer	5
2.2 Gas Absorption	6
2.3 ARTS	8
2.4 HITRAN	9
CHAPTER 3 – MODELS OF CONTINUUM	11
3.1 <i>HITRAN_CIA</i>	11
3.2 <i>MT_CKD</i>	12
CHAPTER 4 – <i>MT_CKD</i> 2.5	17
4.1 Formulation of absorption coefficient in ARTS	18
4.2 H_2O continuum	18
4.2. 1 <i>MT_CKD</i> 1.0 formulation for H_2O self continuum	18
4.2. 2 Changes to H_2O self continuum	19
4.2. 3 <i>MT_CKD</i> 1.0 formulation for H_2O foreign continuum	19
4.2. 4 Changes to H_2O foreign continuum	19
4.3 CO_2 continuum	20
4.3. 1 <i>MT_CKD</i> 1.0 formulation for CO_2 continuum	20
4.3. 2 Changes to CO_2 continuum	20
4.4 N_2 continuum	21
4.4. 1 <i>MT_CKD</i> 1.0 formulation for N_2 CIA rotational band	21
4.4. 2 Changes in N_2 CIA rotational band	21
4.4. 3 <i>MT_CKD</i> 1.0 formulation for N_2 fundamental band	21
4.4. 4 Changes to N_2 fundamental band	22
4.5 O_2 continuum	22
4.5. 1 O_2 fundamental band <i>MT_CKD</i> formulation	22
4.5. 2 O_2 $\nu_0 \leftarrow \nu_0$ band <i>MT_CKD</i> formulation	22
4.5. 3 O_2 $\nu_0 \leftarrow \nu_1$ band <i>MT_CKD</i> formulation	23

CHAPTER 5 – CALCULATION OF ABSORPTION COEFFICIENT AND OUTGOING LONGWAVE RADIATION FLUXES	25
5.1 Outgoing longwave radiation calculation	25
5.2 Basic assumptions and atmospheric scenarios	26
5.3 Absorption coefficient calculation	27
CHAPTER 6 – ANALYSIS OF DIFFERENCES BETWEEN DIFFERENT CONTINUUM MODELS	31
6.1 Comparison between <i>MT_CKD2.5</i> and <i>MT_CKD1.0</i>	31
6.2 Comparison between <i>MT_CKD2.5</i> and <i>HITRAN_CIA</i> model	37
6.3 Comparison between <i>MT_CKD 2.5</i> , <i>MT_CKD 1.0</i> , <i>HITRAN_CIA</i> and line absorption	42
CHAPTER 7 – SUMMARY AND CONCLUSIONS	45

Acknowledgements

I would like to thank my supervisor Jana Mendrok for giving me this opportunity to work with satellite atmospheric science group of Lulea Technical University. Her valuable guidance and scientific inputs have helped me to understand and carry forward my work in ease. I am grateful to Stefan Buehler for discussions and suggestions on my results. Thank you, Mathias Milz, Thomas Kuhn, Richard Larsson, Oliver Lemke, Madhuri Nukala, Anyairo Charles, Mats Wallberg, Jose Ignacio Martinez, Victoria Barabash, Maria Winneback, Anette Snllfot-Brndstrm and Johnny Ejemalm for your help. I would also like to thank Lulea Technical University and Paul Sabatier University for their technical support. I am also grateful to all my friends Astha Singh, Beenish Batul, Christina Sherly, John Panikulam, Manohar Karnal, Florian Trost, Daria Calangiu and Taha Moufid for their support and help.

Abstract

Continuum absorption plays important role in Earth's radiative cooling and energy balance. Its impact on outgoing longwave radiation fluxes is profound, decreasing it by as much as 12 W/m^2 . Molecules contributing to continuum absorption in microwave and infrared region (significant for OLR studies) are water vapour, oxygen, nitrogen, ozone and carbon dioxide. Laboratory measurements of continua of some of these molecules (specially water vapour) is difficult. To overcome this continuum models are developed. These are semiempirical models, considers theoretical information with laboratory and field measurements.

Comparison between two state-of-art continuum models *MT_CKD* (Mlawer-Tobin-Clough-Kneizys) and *HITRAN_CIA* (High resolution TRANsmission databse: Collision Induced Absorption) is discussed to find out their impact on calculation of Outgoing Longwave Radiation (OLR) fluxes and source of uncertainty for climate models. For simulations Atmospheric Radiative Transfer Simulator (ARTS) is used. *MT_CKD* 2.5 is the latest version of *MT_CKD* continuum model. *MT_CKD* 1.0 and *HITRAN_CIA* was already included in ARTS, implementation of *MT_CKD* 2.5 is done in this thesis. Five different atmospheric scenarios (midlatitude summer, midlatitude winter, subarctic summer, subarctic winter and tropical) are considered for comparison studies.

The OLR fluxes calculated using *MT_CKD* 1.0 and latest *MT_CKD* 2.5 gives relative difference of order of 0.01%. So, difference between these two model with respect to OLR calculation is insignificant. But, relative difference between fluxes in some wavenumber region can be as high as 30%, which might be a source of error for studies or instruments using those wavenumber ranges.

Difference between OLR calculated using *MT_CKD* 2.5 and *HITRAN_CIA* is the order of 1%. OLR calculated using only line by line absorption differs by order of 0.01% from *HITRAN_CIA*. *HITRAN_CIA* does not include water vapour continuum, which is major contributor in continuum absorption. OLR values calculated by considering continuum models (in addition to the line by line absorption model) decreases.

CHAPTER 1

Introduction

Earth, which is a home to all living beings, is surrounded by the atmosphere, which plays a big role in their survival. It protects all the organisms from harmful solar radiation and also maintains the temperature. Solar radiation enters the Earth's atmosphere as shortwave radiation, which gets absorbed by Earth and atmosphere. The absorbed energy is emitted as longwave radiation partly from Earth's surface, but significant part from higher levels of atmosphere. Balance between incoming shortwave energy flux and outgoing longwave radiation energy flux governs the radiative energy balance of Earth's atmosphere. Longwave energy radiation flux can be calculated using the absorption properties of the atmosphere [Salby, 1996].

It is important to perform accurate calculation of atmospheric radiative transfer for understanding of the atmospheric processes and for improving performance of general climate models. One of the major factor, which contribute to the atmospheric radiative transfer is the gaseous absorption in the atmosphere. Accuracy of modelling of the gaseous absorption depends on our knowledge of spectroscopy (line parameters, line shape and continuum) [Payne et al., 2011].

In this thesis, main focus is the continuum absorption by atmospheric gases. Continuum absorption impacts critically on the weather and climate of the Earth [Elsasser, 1938]. For example, the radiative effects of water vapour continuum contributes around 40% of the total longwave radiative cooling rate, near the surface [Clough et al., 1992].

In addition to resonant line absorption, some molecular species shows non-resonant continuum absorption. Continuum absorption varies slowly with frequency, which makes it possible to distinguish it from the line absorption. It should be noted that only total absorption can be measured. Exact distinction between line and continuum absorption depends on the model. Generally, continuum term is used to bring the agreement of line by line model with total absorption from experimental data [Buehler et al., 2005].

In the Earth's atmosphere, water vapour, oxygen, carbon dioxide, methane and nitrogen molecules contribute significantly to the continuum absorption [Payne et al.,

2011]. Continuum absorption is handled by empirical models based on laboratory experiments as well as semiempirical models based on field measurements. So, here it decided to use two models; one is collision induced absorption (*CIA*) by High resolution TRANsmision (*HITRAN*) database and other one is Mlawer Tobin Clough Kneizys Davies (*MT_CKD*). To perform the simulations using these models software called Atmospheric Radiative Transfer Simulator (*ARTS*) is used.

There are two objectives implemented in this thesis, which are explained below:

- As *MT_CKD* 1.0 and *HITRAN_CIA* already exist in ARTS, *MT_CKD* 2.5 is included ARTS in form of *C++* code.
- Comparison study of *HITRAN_CIA*, *MT_CKD* 1.0 and *MT_CKD* 2.5 is done with respect to absorption coefficient, flux and OLR, to find out whether this is an important source of uncertainty for climate models.

An outline of the thesis is as follows: Chapter 2 discusses about radiative transfer, absorption and ARTS. In chapter 3, information about continuum models used for comparison studies are given. Implementation details of the *MT_CKD* 2.5 are discussed briefly in chapter 4. Constraints required to generate the results are given in chapter 5. In chapter 6, results are discussed. Conclusion is given in chapter 7.

CHAPTER 2

Background

2.1 Radiative transfer

Radiative transfer is a phenomenon where energy transfer happens in the form of electromagnetic radiation. Here, we are interested in radiative transfer in the Earth's atmosphere. Specific intensity of radiation I_ν is defined as energy flux per unit time, per unit frequency, per unit solid angle and per unit area normal to the direction of propagation. Equation of radiative transfer states that specific intensity of radiation I_ν decreases due to extinction and increases due to emission when propagates through medium that is

$$\frac{1}{-\mu_\nu} \frac{dI_\nu}{dx} = I_\nu - J_\nu \quad (2.1)$$

x is a coordinate along the path, μ_ν is a extinction coefficient and J_ν specific emission coefficient [Goody RM, 1989]. Extinction coefficient μ_ν includes absorption coefficient α_ν and scattering coefficient s_ν .

$$\mu_\nu = \alpha_\nu + s_\nu \quad (2.2)$$

Here we consider only clear sky radiative transfer calculation, where only absorption and emission of the medium, are considered, avoiding the scattering term which usually occurs in the presence of clouds for infrared and microwave wavelengths [Goody RM, 1989].

$$\mu_\nu = \alpha_\nu \quad (2.3)$$

$$J_\nu = B_\nu(T) \quad (2.4)$$

Therefore, transfer equation becomes

$$\frac{dI_\nu}{dx} = -\alpha_\nu I_\nu + \alpha_\nu B_\nu(T) \quad (2.5)$$

$B_\nu(T)$ ($\text{Wsr}^{-1}\text{m}^{-2}\text{Hz}^{-1}$) is the Planck's function.

$$B_\nu(T) = \frac{2h\nu^3}{c^2(e^{h\nu/kT} - 1)} \quad (2.6)$$

$h = 6.63 \times 10^{-34}\text{m}^2\text{kg/s}$ is a Planck's constant, $k = 1.38 \times 10^{-23}\text{m}^2\text{kgs}^{-2}\text{K}^{-1}$ is a Boltzmann's constant and ν is frequency in Hz.

Total absorption at any point in the atmosphere is the addition of absorption by each absorbing species present at that point. For individual absorption there is one more quantity absorption cross-section κ_i (cm^2/mol), absorption coefficient with respect to absorption cross-section is defined here

$$\alpha_i = \kappa_i n_i \quad (2.7)$$

α_i (cm^{-1}) is absorption coefficient from each individual absorber and n_i (mol/cm^3) is number density of absorber. It should be noted that in this thesis, unit of wavenumber is cm^{-1} (=frequency (1/s)/speed of light (cm/s)). Unit of absorption coefficient is also cm^{-1} , here it is referred as per unit distance.

2.2 Gas Absorption

Absorption of electromagnetic radiation is the physical phenomenon, when the energy of the photon is taken up by the matter and converted into internal energy (translational, rotational or vibrational energy). If a photon, of the energy same as the difference in two quantum mechanical state of the molecule, it gets absorbed and molecule changes its state. Table 2.1 gives types of electromagnetic transitions and spectrum where it is significantly happens.

Table 2.1: Types of Transitions

Transitions	Related Spectrum
Electronic	Ultra Violet (UV) and visible
Rotational	microwave
Rotational-vibrational	mid infrared

The absorption that occurs due to transition between two states of a molecule is referred as an absorption line. To calculate absorption over a spectral region, one needs to calculate the contribution of each absorption line for all molecules in the atmospheric layer. This technique is known as line-by-line calculation. Absorption coefficient ($\alpha(\nu)$) for an absorption line can be written as [Salby, 1996]

$$\alpha(\nu) = n S(T) F(\nu) \quad (2.8)$$

n is the number density, $S(T)$ is the line strength and $F(\nu)$ is called as line shape function. For detail discussion of line-by-line calculation see P Eriksson and Lemke [2011].

Some molecules like H_2O , O_2 , N_2 , CH_4 show continuum (broad band background characteristic, which varies slowly with frequency) absorption in addition to the line absorption.

For some molecules, continuum can be defined physically, while for others it is just more or less empirical corrections for deficits in line-by-line calculation. For the later, contribution from a uniform line shape function and spectroscopic parameters of individual line is subtracted from total measured absorption. So, basically continuum depends on selection of line shape function and spectroscopic database [Rothman et al., 2013].

In this thesis, continuum due to water vapour (H_2O), oxygen (O_2), nitrogen (N_2), methane (CH_4) and carbon dioxide (CO_2) are considered. The reason for continuum to occur with respect to these molecules are different, because of differences in permanent electric and magnetic dipole multipole, for details see Goody RM [1989].

Water vapour has strong electric dipole moment, therefore it possess rotational transitions in microwave range. Exact reason for continuum of H_2O is still ambiguous. There are several possibilities like collision-induced absorption, water polymer absorption, contribution of far-infrared water lines in far wings [Rosenkranz, 1998] or inadequate line shape formulation. For inadequate line shape formulation derivation valid only near wing zone [Van Vleck and Weisskopf, 1945].

Water vapour continuum contributes at high rate to the Earth's energy balance, it can be as high as 40 % at the surface of Earth [Mlawer et al., 2012]. At higher altitude its contribution decreases due to decrease in its concentration (see chapter 6). Its impact to the longwave radiation transfer is profound, it decreases OLR fluxes as much as 10 W/m^2 [Mlawer et al., 2012]. So, it is important to study the water vapour continuum.

Symmetrical molecules like oxygen, nitrogen, methane does not possesses permanent electric dipole. These molecules creates transient dipole when involved in collision. Transient or fluctuating dipole induced during collisional interaction of free molecules (for example: O_2-O_2 , O_2-N_2) absorbs radiation known as Collision Induced Absorption (CIA) [Frommhold et al., 1987]. This absorption depends on density of molecules involved in collision. For more details see section 3.1.

O_2 possess permanent magnetic dipole moment. It has $^3\Sigma$ ground state due to aligned spins of two valence electron. As per selection rule for magnetic dipole transitions, with resonance frequency equal to zero transitions are allowed, where these transitions have Debye line shape function [Rosenkranz, 1993].

N_2 is a homonuclear molecule, which has an electric quadruple moment of modest magnitude in lowest order. The electric field due to electric quadruple moment of one molecule induces a dipole moment in the second molecule. This allows rotational transitions as per the electric quadruple selection rule [Rosenkranz, 1993].

Continuum absorption is important in microwave and infrared spectrum of the

atmosphere due to influence of their absorption on the Earth's radiative heat budget and also their effects on remote sensing measurements [Rinsland et al., 1989][Payne et al., 2011]. For example, in the measurement of liquid water path (LWP) for the clouds with low optical depth accurate modelling of continuum absorption is important, because of large contribution of continuum to the total optical depth. These thin liquid water clouds plays important role in determination of Earth's radiative energy balance [Payne et al., 2011].

2.3 ARTS

Atmospheric radiative transfer simulator is an open source software which is used to perform simulations of atmospheric radiative transfer. Radiative transfer simulators are used for developing and designing new sensors, for processing actual measurements to retrieve atmospheric parameters (for example temperature, pressure etc.) or for doing corrections to the measurements of radiation from Earth or space for the influence of contributions from atmosphere. ARTS assumes spherical atmosphere, instead of parallel atmosphere which gives more accurate results [Buehler et al., 2006]. ARTS makes it possible to do calculations in the frequency range of microwave to thermal infrared.

Relative to other radiative transfer softwares, ARTS is general and flexible. It is easy to add new calculations to the ARTS and can be used for wide range of applications. It works as a scripting language. A sequence of instructions are given in an ARTS controlfile when executed, parses the controlfile, and sequence of instructions are executed. Controlfiles contain a list of workspace methods, which perform calculations when executed. Workspace methods take work space variables as inputs and outputs. Workspace variables are physical quantities. It is easy to add new workspace variables and methods because ARTS control files have well-defined syntax.

ARTS has been implemented in the *C++* programming language. It can be installed and used on different Unix and Linux systems with different versions of GNU gcc compiler. ARTS-data is a package which contains spectral line catalogue and atmospheric states, which are in formats suitable for ARTS. CIRA86 [Fleming et al., 1990], FASCOD [Anderson et al., 1986] and REFMOD99 [Rinsland et al., 1991] are atmospheric scenarios included in ARTS-data. ARTS has its own spectral line data, as well as it can also use JPL [Pickett et al., 1998], HITRAN [Rothman et al., 2013] (are spectral line catalogues). In this thesis, FASCOD atmospheric scenarios and HITRAN spectral line catalogue are used.

To calculate the total absorption, one need to define absorption species with their tags in control file. Tags are stored in a variable called 'abs_species' in the control file. Tags of these gaseous absorption species specify the considered absorber, model that it uses to calculate absorption coefficient. Types of tags and their examples are given in Table 2.2. It should be noted that we can specify, any combination of tags of absorption species in control file. In this thesis, line-by-line absorption species are used with continuum absorption species to calculate the total absorption.

Table 2.2: Absorption species tags

Types	Example	Explanation
Line-by-line	H2O-18	line-by-line calculation of H_2O with particular isotopologue
Continuum	H2O-SelfContCKDMT100	H_2O self continuum using <i>MT_CKD</i> (For details see 4)
Complete	H2O-PWR98	H_2O complete model P Eriksson and Lemke [2011]
Zeman effect	O2-Z	O_2 with Zeeman effect P Eriksson and Lemke [2011]

2.4 HITRAN

High resolution TRANsmission (HITRAN) a molecular absorption database. It is used to predict the light emission and transmission by many computer codes. The HITRAN compilation contains several components, for details see Rothman et al. [2013]. Here, we are interested in line-by-line spectroscopic parameters and collision induced dataset. Collision induced dataset is discussed in section 3.1. HITRAN line-by-line spectroscopic parameters for calculation of high resolution absorption and radiance are available from microwave to visible spectrum. At this point, there are 47 species and respective 109 isotopologues.

In this thesis, HITRAN spectroscopic database is used for line-by-line (LBL) calculation. For OLR calculation H_2O , CO_2 , O_3 , N_2O , CO , CH_4 , O_2 , NO , NO_2 , HNO_3 and N_2 , these species are relevant (for details see Buehler et al. [2005]).

CHAPTER 3

Models of Continuum

3.1 *HITRAN_CIA*

Collision induced absorption (CIA) is caused by symmetric molecules, such as O_2 , N_2 , H_2 and CH_4 . These kind of molecules do not possess a dipole moment in isolated states. When involved in collisions they may have dipole moment induced in it. In that case dipole transitions may occur in short duration of collision. Above mentioned molecules possess high degree of symmetry, so transition is forbidden by selection rule. Forbidden transitions are the transitions (here it means magnetic dipole or electric quadruple transitions) which are less likely to occur, compared to permitted transitions by selection rule (for details see Goody RM [1989]). If that symmetry gets destroyed during a collision, a transition may happen leading to absorption. Amount of absorption due to binary CIA is dependent on the density of both molecules involved in collision. Absorption due to CIA plays a large role in total radiation absorption [Solomon et al., 1998], that's why it is a very important factor in the modelling of radiative transfer of the Earth's atmosphere.

Here, we have decided to use binary (involving only two molecules) absorption cross section for CIA offered by HITRAN catalogue [Richard et al., 2012] in tabular form. The data of collision induced absorption provided by HITRAN is obtained by pure laboratory measurements, semi-empirical models and theoretical calculations [Frommhold, 2006]. It should be noted that, at this point collision induced absorption offered by HITRAN only comprises binary absorption. Knowledge of absorption involving three or more molecules is limited and not included in HITRAN [Richard et al., 2012].

HITRAN collision induced absorption data is incorporated in ARTS with following variables. Absorption coefficient $\alpha_{i,j}$ (cm^{-1}) is calculated from binary absorption cross-section $k_{i,j}$ ($\text{cm}^5\text{mol}^{-2}$) by multiplying it with the number densities n_i and n_j ($\text{mol}/\text{cm}^{-3}$) of the both molecules involved in collision. It should be noted that unit of absorption is per distance ($1/\text{cm}$).

$$\alpha_{i,j} = k_{i,j} n_i n_j \quad (3.1)$$

i and j represents the two involved species. When compared to Equation 2.7, it can be observed that Equation 2.7 is for single molecule, while Equation 3.1 is for two involved molecules.

3.2 *MT_CKD*

As mention in section 2.2, contribution of water vapour continuum to the longwave radiation of Earth is very high. (*MT_CKD*) [Mlawer et al., 2012] is introduced for radiative transfer modelling involving water vapour continuum.

MT_CKD has been developed with the assumption that water continuum occurs due to the interaction between water molecule with other water molecule (self continuum or self-broadened continuum) or a different molecule (foreign continuum or foreign broadened continuum). MT_CKD uses semi-empirical approach, where Van Vleck and Huber (VVH) line shape formalism is incorporated, which is modified using χ -function to be consistent with observations. Here, semi-empirical means a known physical mechanism is incorporated into the adopted formalism with an objective, to attain agreement between measured and derived values. Line shape formulation for calculation of absorption coefficient $k(\nu)$ (cm^2/mol) is given by

$$k(\nu) = R(\nu) \sigma(\nu) \quad (3.2)$$

$$R(\nu) = \nu \tanh(\beta\nu/2) \quad (3.3)$$

ν (cm^{-1}) is wavenumber. $R(\nu)$ (cm^{-1}) is the radiation field term at temperature T with $\beta = hc/kT$. It includes the effect of stimulated emission, for details see Clough et al. [1989]. σ (cm^3/mol) symmetrized power spectral density function.

$$\sigma(\nu) = \sum_i \tilde{S}_i(T) \frac{1}{\pi} \left[\frac{\alpha_i}{(\nu - \nu_i)^2 + \alpha_i^2} \chi(\nu - \nu_i) + \frac{\alpha_i}{(\nu + \nu_i)^2 + \alpha_i^2} \chi(\nu + \nu_i) \right] \quad (3.4)$$

where \tilde{S}_i (cm^2/mol) is the intensity of transition at wavenumber ν_i and of halfwidth α_i . $\alpha_i = \alpha_i^0(\rho/\rho_0)$ and α_i^0 is the self-broadened half-width at the atmospheric density ρ_0 , is of the order of 0.1 cm^{-1} (0.5 cm^{-1} for self-broadened water vapour) [Clough et al., 1989].

$$L(\nu - \nu_i) = \frac{1}{\pi} \frac{\alpha_i}{(\nu - \nu_i)^2 + \alpha_i^2} \quad (3.5)$$

is the Lorentz line function, while χ function is multiplied to line function to attain the agreement between calculated and measured spectra. At $\chi = 1$, Lorentz function in Equation 3.5 corresponds to the impact approximation. To attain agreement between calculated and measured spectra, χ semi-empirical function is applied to impact approximation. Continuum absorption is obtained by excluding local line

contribution (which is defined for each line within $\pm 25\text{cm}^{-1}$ from the center line) from power spectral density function.

$$\tilde{C}(\nu) = \sum_i \tilde{S}_i [L_c(\nu - \nu_i) \chi(\nu - \nu_i) + L_c(\nu + \nu_i) \chi(\nu + \nu_i)] \quad (3.6)$$

where $L_c(\nu - \nu_i)$ is the Lorentz line shape with the intensity peak at the line center removed and is a function of wave number ν_i . $L_c(\nu \pm \nu_i)$ is systematically defined as follows

$$L_c(\nu \pm \nu_i) = \begin{cases} \frac{1}{\pi} \frac{\alpha_i}{25^2 + \alpha_i^2} & |\nu \pm \nu_i| \leq 25\text{cm}^{-1} \\ \frac{1}{\pi} \frac{\alpha_i}{(\nu \pm \nu_i)^2 + \alpha_i^2} & |\nu \pm \nu_i| \geq 25\text{cm}^{-1} \end{cases} \quad (3.7)$$

Here, it is important to mention that χ function for self- and foreign continuum is defined separately (for detail discussion see Clough et al. [1989]). χ for self continuum (χ_s) is dependent on temperature, while for foreign continuum (χ_f) is independent of temperature. For pragmatic purposes, extrapolation technique is used to calculate χ_s . χ_s is calculated at 296 K and 338 K using least-squares fitting and is extrapolated at required temperature. For reliability of this technique see Clough et al. [1989]. As mentioned in section 2.2, one of the reason behind existence of water vapour continuum can be inadequate line shape. So, continuum depends on the details of line-by-line calculation. *MT_CKD* model is consistent with FASCODE line-by-line model [Smith et al., 1978].

In *MT_CKD* formulation, collision induced and allowed transitions terms are present in self- and foreign continuum [Payne et al., 2011]. Collision induced term provides the excess absorption observed in the central region of vibrational band. The continuum behaviour between water vapour bands obtained from measurement is less than that associated with the far wing behaviour of the Lorentz line shape known as sub-Lorentzian shape. For allowed transition, a second line shape is applied to each allowed water vapour line to provide sub-Lorentzian shape.

As mentioned above, in *MT_CKD* model continuum is a sum of 'allowed' and 'weak interaction' terms. Equations 3.6-3.7 gives allowed term, with χ is defined as follows

$$\chi(\nu \pm \nu_i) = \begin{cases} 1 + [\chi'(\nu \pm \nu_i) - 1] \frac{25^2}{(\nu \pm \nu_i)^2 + \alpha_i^2} & |\nu \pm \nu_i| \leq 25\text{cm}^{-1} \\ \chi'(\nu \pm \nu_i) & |\nu \pm \nu_i| \geq 25\text{cm}^{-1} \end{cases} \quad (3.8)$$

χ' and weak interaction formulation is separate for self continuum (χ'_s) and foreign continuum (χ'_f).

MT_CKD self continuum χ'_s is

$$\chi'_s(\nu \pm \nu_i) = \left(1 + \frac{|\nu \pm \nu_i|}{\gamma_a}\right) \exp\left(-\frac{|\nu \pm \nu_i|}{\gamma_a}\right), \quad \gamma_a = 61.5\text{cm}^{-1} \quad (3.9)$$

MT_CKD self continuum weak interaction term is

$$\Sigma_i \frac{\tilde{S}_i \alpha_{WI} / \pi}{\alpha_{WI}^2 + (\nu - \nu_i)^2} \left\{ \zeta_{i,WI} \exp \left[- \left(\frac{\nu - \nu_i}{\gamma_{WI}} \right)^2 \right] \right\} \quad (3.10)$$

$$\alpha_{WI} = 70.09 \text{cm}^{-1} \quad \gamma_{WI} = 54.05 \text{cm}^{-1}$$

MT_CKD foreign continuum χ'_f is

$$\chi'_f(\nu \pm \nu_i) = \exp \left[- \left(\frac{|\nu \pm \nu_i|}{\gamma_a} \right)^{p_a} \right], \quad p_a = 1.462 \text{cm}^{-1}, \quad \gamma_a = 310.5 \text{cm}^{-1} \quad (3.11)$$

MT_CKD self continuum weak interaction term is

$$\Sigma_i \frac{\tilde{S}_i \alpha_{WI} / \pi}{\alpha_{WI}^2 + (\nu - \nu_i)^2} \left\{ \zeta_{i,WI} \exp \left[- \left(\frac{\nu - \nu_i}{\gamma_{WI}} \right)^2 \right] \right\} \quad (3.12)$$

$$\alpha_{WI} = 87.72 \text{cm}^{-1} \quad \gamma_{WI} = 306.6 \text{cm}^{-1}$$

In weak interaction, term for self- and foreign continuum, sum is over all i (species) with strength \tilde{S}_i and position ν_i . The relative strength of interaction $\zeta_{i,WI}$ depends on lower energy state and rotational quantum number, and taken from spectral line catalogue. This term is same for self- and foreign continuum. For detail formulation see Mlawer et al. [2012].

MT_CKD is a semiempirical model, where fitting has been done using laboratory and atmospheric measurements while it is strongly constrained by the known physics. Only highly scrutinized atmospheric cases have been used, while in the region where measurements have not been tested, mathematical shape of each monomer (is a molecule which may bind to other molecule to form polymer) line has been developed. *MT_CKD* model can be applied from microwave to visible region, to study the continuum absorption for water vapour (H_2O), carbon dioxide (CO_2), nitrogen (N_2), oxygen (O_2) and ozone (O_3). To be consistent with current observational studies, some periodic updates have been done to *MT_CKD* model. Major developments in *CKD* and *MT_CKD* models is mentioned in Table 3.1

Table 3.1: Models and release dates

Model	Date	Changes
<i>MT_CKD</i> 2.5.2	January 2011	Changes mentioned in chapter 4
<i>MT_CKD</i> 1.0	February 2003	New formulation
<i>CKD</i> 0	1989	First <i>CKD</i> continuum model released

Until now, we have discussed about parametrization of water vapour continuum in *MT_CKD*, but with water vapour, *MT_CKD* also includes continuum formulation

of carbon dioxide (CO_2), nitrogen (N_2), oxygen (O_2) and ozone (O_3). CO_2 continuum parametrization is somewhat analogous to H_2O continuum parametrization. The major difference is line contribution within $\pm 25\text{cm}^{-1}$. For CO_2 continuum, a first-order treatment of CO_2 line coupling constructed using Lamouroux et al. [2010] databases and software using P, Q and R branches. The line contribution within $\pm 25\text{cm}^{-1}$ of line center is reduced by above function to preserve the total absorption. To calculate the continuum parameter, above mentioned base line function is combined with all the contributions from the wings of all lines. These parameters are calculated at 296K and stored in tabular form which is used in *MT_CKD* model. For more details see [Mlawer et al., 2012]. Formulation of absorption coefficient using this parameter is discussed in chapter 4.

For N_2 and O_2 continuum, parametrization is taken from other sources and further calculation is done in *MT_CKD* model. For N_2 collision induced rotational band continuum (parameters taken from Borysow and Frommhold [1986]) and collision induced fundamental continuum (parameters taken from Lafferty et al. [1996]) has been considered in *MT_CKD*. For O_2 collision induced fundamental band (parameters taken from Thibault F [1997]), O_2 $\nu_0 \leftarrow \nu_0$ band (parameters taken from Maté et al. [1999]) and O_2 $\nu_0 \leftarrow \nu_1$ (parameters taken from Mlawer et al. [1998]) has been considered. O_3 continuum is not discussed in this thesis.

CHAPTER 4

MT_CKD 2.5

There has been a number of well-founded measurements, after the release of *MT_CKD* 1.0, which provided more accurate continuum absorption coefficients in certain spectral regions, which have indicated changes in absorption coefficient in those spectral regions. To incorporate those changes revisions of *MT_CKD* 1.0 models have been released as mentioned in Mlawer et al. [2012]. ARTS has *MT_CKD* 1.0 included in it. In this thesis, *MT_CKD* 2.5 has been included in ARTS.

To include *MT_CKD* 2.5 in ARTS, *MT_CKD* 2.5 FORTRAN code (from EJ Mlawer) has been studied. After comparing *MT_CKD* 2.5 FORTRAN code and *MT_CKD* 1.0 in ARTS, we realised that it is possible to use *MT_CKD* 1.0 in ARTS as reference and then with some modifications *MT_CKD* 2.5 can be added to ARTS. Here, those changes have been discussed. *MT_CKD* 2.5 FORTRAN code includes continuum of H_2O , CO_2 , O_3 , O_2 and N_2 . O_3 is not included, because of limited time frame.

Continuum of H_2O , CO_2 , O_2 and N_2 has been divided into different parts depending on their properties, for details see Goody RM [1989]. Molecules and there continuum parts (here mentioned as species) are discussed in Table 4.1.

Table 4.1: Continuum Species

Molecule	Continuum species	Wavenumber range cm^{-1}
H_2O	Self Continuum	0-20000
	Foreign Continuum	0-20000
CO_2	CO_2 continuum	0-10000
N_2	CIA rotational band continuum	0-350
	CIA fundamental band continuum	2085-2670
O_2	CIA fundamental band continuum	1340-1850
	$\nu_0 \leftarrow \nu_0$ band continuum	7536-8500
	$\nu_0 \leftarrow \nu_1$ band continuum	9100-11000

4.1 Formulation of absorption coefficient in ARTS

To calculate continuum absorption coefficient for each continuum segment mentioned in Table 4.1 following formula has been used.

$$\alpha(\nu) = VMR_{mol} n_0 \left(\frac{P}{P_0} \frac{T_0}{T} \right) \left(\frac{P}{P_0} \frac{T_1}{T} \right) C_{mol} R(\nu) \quad (4.1)$$

where VMR_{mol} is volume mixing ratio of the molecule, $n_0 = 2.687 \times 10^{25} \text{ mol/cm}^3$ is the Loschmit number, P and T are ambient pressure and temperature respectively. $P_0 = 1013 \text{ hPa}$, $T_0 = 273 \text{ K}$, T_1 is the temperature related to C_{mol} . C_{mol} is the continuum parameter of the species. After, going through *MT_CKD* 2.5 FORTRAN code and comparing it with *MT_CKD* 1.0 in ARTS, it has been observed that C_{mol} in *MT_CKD* 1.0 should be modified to incorporate the changes. $R(\nu)$ is a radiation field term, for explanation see chapter 3. According to ideal gas law,

$$N_{mol} = VMR_{mol} n_0 \left(\frac{P}{P_0} \frac{T_0}{T} \right) \quad (4.2)$$

N_{mol} is the number density of the molecule at ambient pressure P and temperature T . Therefore, Equation 4.3 can be written as

$$\alpha(\nu) = N_{mol} \left(\frac{P}{P_0} \frac{T_1}{T} \right) C_{mol} R(\nu) \quad (4.3)$$

4.2 H_2O continuum

For detail formulation of H_2O continuum, see chapter 3. The relation between formulation in chapter 3 and equation 4.3 is discussed below. Comparing equations 2.7, 3.2 and 4.3, we can say

$$\tilde{C} = N_{mol} \left(\frac{P}{P_0} \frac{T_1}{T} \right) C_{mol} \quad (4.4)$$

H_2O self and foreign continuum formulation in *MT_CKD* 1.0 ARTS code and changes done to include *MT_CKD* 2.5 H_2O continuum is discussed in this section.

4.2. 1 *MT_CKD* 1.0 formulation for H_2O self continuum

H_2O self continuum parameter C_{s,H_2O} at temperature 296 K ($C_{s,H_2O,296}$) and 260 K ($C_{s,H_2O,260}$) is available in the table format for wavenumber of the range $0-20000 \text{ cm}^{-1}$ at the interval of 10 cm^{-1} . It should be noted that C_{s,H_2O} depends on temperature. So, C_{s,H_2O} at ambient temperature is calculated by interpolating $C_{s,H_2O,296}$ and $C_{s,H_2O,260}$ with respect to temperature, formulated as follows

$$T_{fac} = \frac{T - T_0}{260 - T_0} \quad (4.5)$$

$$C_{s,H_2O} = C_{s,H_2O,296} \left(\frac{C_{s,H_2O,260}}{C_{s,H_2O,296}} \right)^{T_{fac}} \quad (4.6)$$

For wavenumber of range $820 - 960\text{cm}^{-1}$, C_{s,H_2O} is multiplied by correction factor.

4.2. 2 Changes to H_2O self continuum

Modification to self continuum in microwave range and in far-infrared range has been done to provide agreement with measurements. Measurements in microwave range has been done using two channel microwave radiometers (23.8 GHz or 0.8 cm^{-1} and 31.4 GHz or 1.05 cm^{-1}) [Payne et al., 2011], while measurements in far-infrared has been done in first phase of Radiative Heating in Under explored Bands Campaigns (RHUBC) [Delamere et al., 2010].

To incorporate above changes Equation 4.6 is changed as follows

$$C_{s,H_2O} = C_{s,H_2O,296} \left(\frac{C_{s,H_2O,260}}{C_{s,H_2O,296}} \right)^{T_{fac}} \left(1 + \left[\frac{0.25}{1 + \left(\frac{\nu}{350} \right)^6} \right] \right) \quad (4.7)$$

There is a big difference between self continuum coefficient calculated using *MT_CKD* 1.0 and laboratory measurements in near-infrared region ($2000 - 3000\text{cm}^{-1}$) as presented by Burch and Alt [1984]. To get consistent results for laboratory measurements of Bicknell and Flusberg [2006] and Fulghum and Tilleman [1991] a correction factor [Mlawer et al., 2012] is multiplied to Equation 4.7 for the wavenumber of the range $2000 - 3000\text{cm}^{-1}$.

4.2. 3 *MT_CKD* 1.0 formulation for H_2O foreign continuum

H_2O foreign continuum parameter C_{f,H_2O} valid at all temperatures is available in table format (taken from *MT_CKD* 1.0 FORTRAN code) for wavenumber of the range $0 - 20000\text{cm}^{-1}$ at the interval of 10cm^{-1} [Mlawer et al., 2012].

4.2. 4 Changes to H_2O foreign continuum

Modification of foreign continuum in microwave and far infrared range is to incorporate measurements done as mentioned in Payne et al. [2011] and Delamere et al. [2010]. Modification in $250 - 550\text{cm}^{-1}$ region has been based on analyses of Northern Slope of Alaska data Knuteson et al. [2004]. To incorporate above changes, C_{f,H_2O} is

multiplied by the factor as given below

$$fac = 1 - \frac{0.0252}{1 + 0.3 \left(\frac{\nu}{57.83} \right)^8} \left(\frac{240^2}{(\nu - 255.67)^2 + 240^2 + \left(\frac{\nu - 255.67}{57.83} \right)^8} + \frac{240^2}{(\nu + 255.67)^2 + 240^2 + \left(\frac{\nu + 255.67}{57.83} \right)^8} \right) \quad (4.8)$$

4.3 CO_2 continuum

4.3. 1 MT_CKD 1.0 formulation for CO_2 continuum

CO_2 continuum parameter C_{CO_2} [Ridgway et al., 1982] valid at all temperatures is available in table format for wavenumber of the range $0 - 10000\text{cm}^{-1}$ at the interval of 10cm^{-1} .

4.3. 2 Changes to CO_2 continuum

The entire recalculation of CO_2 continuum parameter has been developed, for being consistent with newly implemented line shape formulation [Lamouroux et al., 2010], where first order line coupling of P, Q and R branches of CO_2 bands are considered. So, continuum parameter C_{CO_2} has been completely replaced.

Modification of continuum parameter in the wavenumber range of $2000 - 3200\text{cm}^{-1}$ has been done by multiplying a scaling factor (SF), which has been calculated using Knuteson et al. [2004].

At wavenumber 2385cm^{-1} ν_3 band of CO_2 shows an interesting feature called 'bandhead' [Mlawer et al., 2012]. Comparison with line-by-line radiative transfer model (LBLRTM) [Clough et al., 2005] added with the measurements of other instruments Knuteson et al. [2004] and Aumann et al. [2003] in wavenumber range of $2385 - 2600\text{cm}^{-1}$, showed that need to revise the MT_CKD model by considering temperature dependence of absorption coefficient in this range. Temperature dependence of continuum coefficient in $2385 - 2436\text{cm}^{-1}$ is incorporated by multiplying following term to the C_{CO_2}

$$\left(\frac{T}{T_1} \right)^{TC(\nu)} \quad (4.9)$$

$T_1 = 246\text{k}$, TC is temperature coefficient which is a function of ν .

4.4 N_2 continuum

Nitrogen molecule shows two important continuums: collision induced rotational band continuum and collision induced fundamental continuum, for details see Goody RM [1989].

4.4. 1 *MT_CKD 1.0* formulation for N_2 CIA rotational band

N_2 collision induced rotational band continuum parameters $C_{r,N_2,296}$ at temperature 296K and $C_{r,N_2,220}$ at temperature 220K is available in table format for wavenumber range of $0 - 350\text{cm}^{-1}$ at the interval of 5cm^{-1} [Borysow and Frommhold, 1986]. C_{r,N_2} is a temperature dependent parameter is calculated by interpolating as follows

$$T_{fac} = \frac{T - T_0}{220 - T_0} \quad (4.10)$$

$$C_{r,N_2} = C_{r,N_2,296} \left(\frac{C_{r,N_2,220}}{C_{r,N_2,296}} \right)^{T_{fac}} \quad (4.11)$$

4.4. 2 Changes in N_2 CIA rotational band

In N_2 pure rotation band, to include the effect of $N_2 - O_2$ and $N_2 - N_2$ Boissoles et al. [2003], scaling factors sf_{296} and sf_{220} have been included for the same frequency range as continuum parameter. As, scaling factor is also temperature dependent, it has also been interpolated. To incorporate above mentioned effect C_{r,N_2} has been modified as follows

$$C_{r,N_2} = C_{r,N_2,296} \left(\frac{C_{r,N_2,220}}{C_{N_2,296}} \right)^{T_{fac}} sf_{296} \left(\frac{sf_{220}}{sf_{296}} \right)^{T_{fac}} \quad (4.12)$$

T_{fac} is same as in equation 4.10.

4.4. 3 *MT_CKD 1.0* formulation for N_2 fundamental band

N_2 collision induced absorption fundamental band continuum parameter C_{f,N_2} , valid at all temperatures and temperature coefficient C_{f,N_2t} is available in table format, for wavenumber of range $2085 - 2670\text{cm}^{-1}$, at the interval of 5cm^{-1} taken from Lafferty et al. [1996]. It should be noted that the formulation for absorption coefficient for this continuum, is slightly different as discussed below

$$\alpha(\nu) = \left(\frac{P}{P_0} \frac{T_0}{T} \right)^2 \frac{1}{VMR_{N_2}} \left(0.8387 - 0.0754 \frac{T}{T_0} \right) C_{f,N_2}(\nu) \exp \left(C_{f,N_2t}(\nu) \left(\frac{1}{T_0} - \frac{1}{T} \right) \right) / \nu \quad (4.13)$$

n_0 is Loschmit number and $k(\nu) \neq 0$ only if volume mixing ratio of N_2 ($VMR_{N_2} > 1e - 25$).

4.4. 4 Changes to N_2 fundamental band

Nitrogen collision induced fundamental absorption band, centred at approximately 2330cm^{-1} based on the highly accurate formulation by Lafferty et al. [1996], includes temperature dependence and the varying efficiencies of nitrogen and oxygen molecules as collision partners, with the absorbing nitrogen molecule.

$$\alpha(\nu) = n_0 \left(\frac{P}{P_0} \frac{T_0}{T} \right)^2 (vmr_{N_2} + a_{O_2} vmr_{O_2} + a_{H_2O} vmr_{H_2O}) C_{f,N_2} R(\nu) \left(\frac{C_{f,N_2t}}{C_{f,N_2}} \right) \frac{\frac{1}{T} - \frac{1}{272}}{\frac{1}{228} - \frac{1}{272}} \quad (4.14)$$

$a_{O_2} = 1.294 - 0.4545 \left(\frac{T}{296} \right)$ it represents the relative broadening efficiency of O_2 , $a_{H_2O} = 1$, it represents the relative broadening efficiency of H_2O .

4.5 O_2 continuum

Oxygen molecule shows three collision induced band in infrared regions. First is collision induced fundamental band and other two are categorised according to their vibration transitions, O_2 $v_0 \leftarrow v_0$ band and O_2 $v_0 \leftarrow v_1$ band for details see Goody RM [1989]. Formulation for all the three species is not similar, to that mentioned in equation 4.3. Therefore, formulation of absorption coefficient is discussed here.

4.5. 1 O_2 fundamental band MT_CKD formulation

Continuum parameter C_{f,O_2} , valid at all temperature and temperature coefficient C_{f,O_2t} for fundamental band is available in the wavenumber range of $1340 - 1850\text{cm}^{-1}$ [Thibault F, 1997]. The formulation is as follows

$$\alpha(\nu) = \left(\frac{P}{P_0} \frac{T_0}{T} \right)^2 C_{f,O_2} \exp \left(C_{f,O_2t} \left(\frac{1}{T_0} - \frac{1}{T} \right) \right) \frac{1}{\nu} R(\nu) \quad (4.15)$$

$R(\nu)$ is the radiation field term.

4.5. 2 O_2 $v_0 \leftarrow v_0$ band MT_CKD formulation

Continuum parameter C_{v_0,O_2} is valid at all temperatures. Absorption cross section due to O_2 $v_0 \leftarrow v_0$ band is calculated over wavenumber range of $7536 - 8500\text{cm}^{-1}$ [Maté et al., 1999]

$$\alpha(\nu) = \frac{vmr_{O_2} + 0.3vmr_{N_2}}{0.446} \left(\frac{P}{P_0} \frac{T_0}{T} \right)^2 C_{v_0,O_2} R(\nu) \quad (4.16)$$

$R(\nu)$ is the radiation field term.

4.5.3 O_2 v0←v1 band *MT_CKD* formulation

O_2 v0←v1 band absorption is formulated in the wavenumber range of 9100–11000 cm^{-1} . This formulation is similar to equation 4.3, where C_{v1,O_2} calculated as follows, taken from Mlawer et al. [1998].

$$C_{v1,O_2} = 0.31831 \left(\frac{\frac{1.66e - 4DAMP_1}{HW_1}}{1 + \left(\frac{D\nu_1}{HW_1}\right)^2} + \frac{\frac{3.086e - 5DAMP_2}{HW_2}}{1 + \left(\frac{D\nu_2}{HW_2}\right)^2} \right) \frac{1.053}{\nu} \quad (4.17)$$

$$D\nu_1 = \nu - \nu_{1osc}, \quad D\nu_2 = \nu - \nu_{2osc}$$

$$DAMP_1 = \begin{cases} 1 & D\nu_1 \geq 0 \\ \exp\left(\frac{D\nu_1}{176}\right) & D\nu_1 < 0 \end{cases}$$

$$DAMP_2 = \begin{cases} 1 & D\nu_2 \geq 0 \\ \exp\left(\frac{D\nu_2}{176}\right) & D\nu_2 < 0 \end{cases}$$

$$\nu_{1osc} = 9375\text{cm}^{-1}, \quad \nu_{2osc} = 9439\text{cm}^{-1}, \quad HW_1 = 58.96, \quad HW_2 = 45.04$$

Calculation of Absorption Coefficient and Outgoing Longwave Radiation Fluxes

In this chapter, we are discussing formulation for Outgoing Longwave Radiation (OLR) fluxes, assumptions and atmospheric scenarios used for generating results. Comparison study of absorption models mentioned in this thesis is done using flux, absorption coefficient and OLR fluxes.

5.1 Outgoing longwave radiation calculation

The upwelling radiative flux F_ν^+ ($\text{Wm}^{-2}\text{Hz}^{-1}$) is given by

$$\begin{aligned} F_\nu^+(z) &= 2\pi \int_0^1 I(z, \mu) \mu d\mu \\ &= 2\pi \int_{\pi/2}^\pi I(\theta) \cos \theta \sin \theta d\theta \end{aligned} \tag{5.1}$$

θ is the zenith angle. Monochromatic radiance I_ν ($\text{Wm}^{-2}\text{Hz}^{-1}\text{sr}^{-1}$) is calculated using ARTS, for details see Buehler et al. [2005]. Total upwelling radiative flux, which is integrated over frequency is also known as outgoing longwave radiation, calculated as follows.

$$F^+(z) = \int F_\nu^+(z) d(\nu) \tag{5.2}$$

Plot of flux ($\text{Wm}^{-2}\text{Hz}^{-1}$) vs wavenumber for mid-latitude summer case is plotted in Figure 5.1. This figure gives the general idea of how flux vs wavenumber plot looks like.

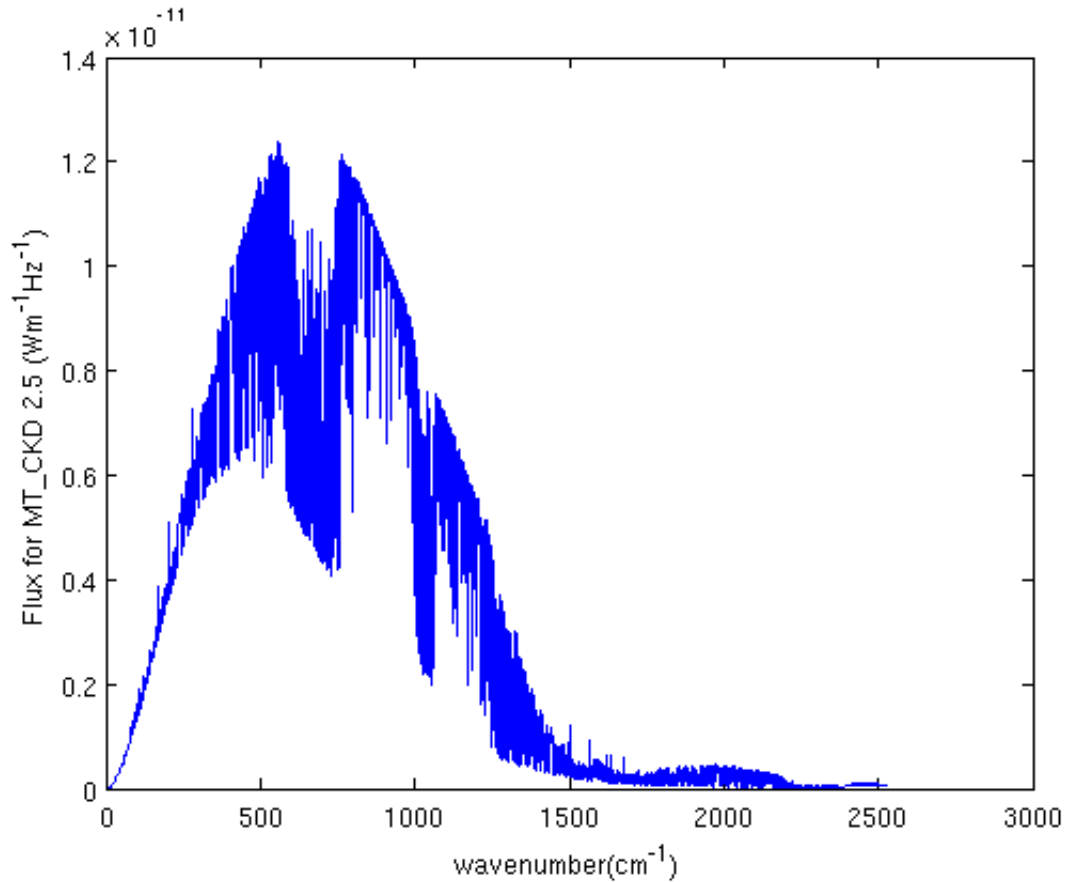


Figure 5.1: Flux at the top of the atmosphere vs wavenumber plot for mid-latitude summer scenario. It should be noted that fluxes are calculated per frequency in Hz, while plotted over wavenumber (by dividing frequency by 3×10^{10} cm/s) for to be consistent with literature.

5.2 Basic assumptions and atmospheric scenarios

Here, all basic assumptions and atmospheric scenarios are referred from Buehler et al. [2006]. In this paper, detail discussion of efficient settings (frequency grid, altitude, atmospheric scenarios, etc.) to calculate OLR fluxes (for comparison study) using ARTS is given.

ARTS is used to perform detailed line-by-line radiative transfer calculation. Five different FASCOD scenarios [Anderson et al., 1986]: midlatitude summer, midlatitude winter, subarctic summer, subarctic winter and tropical are considered . Wavenumber range of $0 - 2525 \text{ cm}^{-1}$ is considered. All the calculation in the ARTS is done by considering frequency in Hz. By converting wavenumber into frequency ($1 \text{ Hz} = 1 \text{ cm}^{-1} \times 3 \times 10^{10} \text{ cm/s}$), we get the frequency range of 0-75750 GHz. This frequency range is divided into equidistant grid of 10000 points for calculation. Although, clouds are having big impact on radiative transfer, but for current studies only clear-sky cases

are considered. At 95km top of the atmosphere is considered, because data is available upto 95km only. ARTS can use different spectroscopic catalogues like JPL [Pickett et al., 1998] and HITRAN [Rothman et al., 2013], but here HITRAN spectroscopic database is used. Species relevant for OLR calculation are H_2O , CO_2 , O_3 , N_2O , CH_4 , CO , O_2 , NO , NO_2 , HNO_3 and N_2 considered for studies in this thesis. Difference in OLR calculation between all HITRAN species and only species mentioned above is less than 0.01% [Buehler et al., 2006]. For zenith angle range of $90^0 - 180^0$ equidistant grid of 40 points is considered which gives accuracy of 0.1%.

Temperature profile for midlatitude summer case is plotted in Figure 5.2. From this figure we can observe the temperature variation along the altitude.

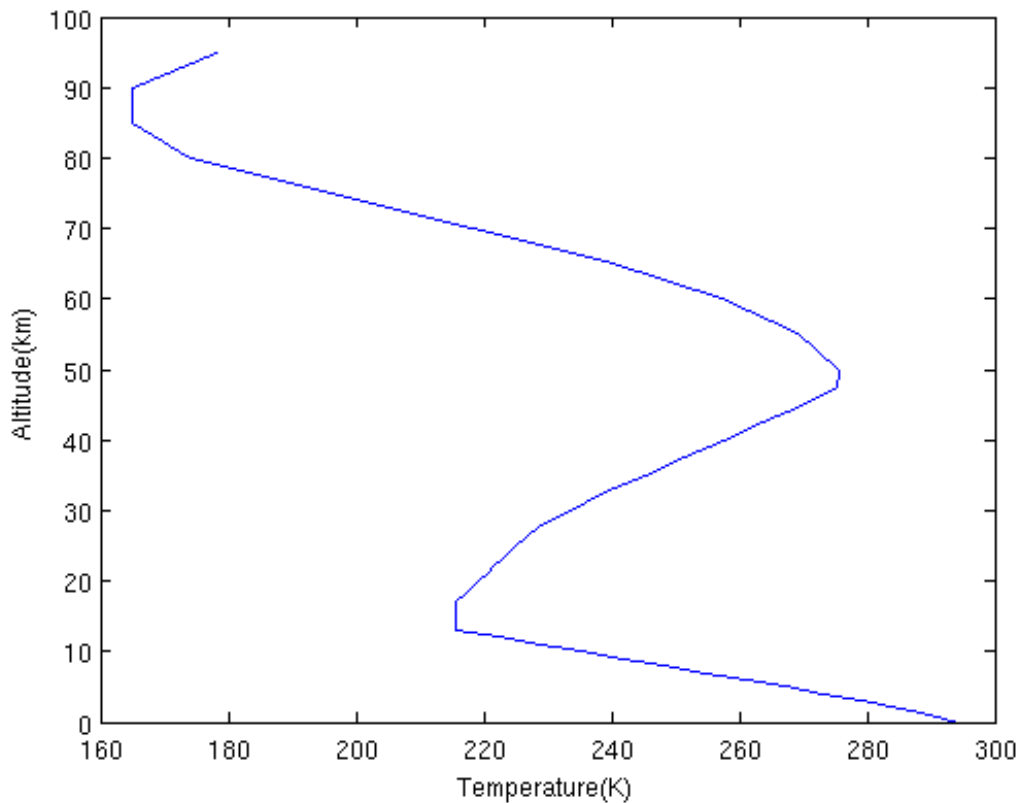


Figure 5.2: Temperature profile for midlatitude summer case

5.3 Absorption coefficient calculation

Total absorption is calculated by adding all the partial absorption of all the absorbers. Partial absorption for the gases which have spectral lines is calculated by adding absorption of each spectral line plus continuum terms (which is more or less

empirical). Details of absorption coefficient calculation in ARTS see Buehler et al. [2005]. Continuum absorption for species H_2O , CO_2 , N_2 and O_2 are considered for two models *MT_CKD* 1.0 and *MT_CKD* 2.5. *MT_CKD* 1.0 was already included in ARTS earlier. *MT_CKD* 2.5 is included in ARTS in this thesis, from FORTRAN code by Mlawer, Tobin, Clough, Kneizys, and Davies Mlawer et al. [2012]. Changes from *MT_CKD* 1.0 to *MT_CKD* 2.5 are explained in chapter 4. *HITRAN_CIA* is calculated for O_2 , N_2 , CH_4 and CO_2 , details are explained in section 3.1. Basically, here absorption coefficients for four different models are calculated

- Line by line (LBL)
- LBL + *MT_CKD* 1.0
- LBL + *MT_CKD* 2.5
- LBL + *HITRAN_CIA*

Species tags (see section 2.3 for explanation) related to above models (which are relevant for this thesis) as they are used in ARTS is mentioned in Table 5.1 with their frequency ranges.

Table 5.1: Absorption Species. It should be noted that there was no change in O_2 continuum from *MT_CKD* 1.0 to *MT_CKD* 2.5. So, O_2 continuum species for *MT_CKD* 2.5 are same as *MT_CKD* 1.0

Absorption Model	Species Tags	Waveno. Range (cm ⁻¹)	Description
Line	H2O, O2, N2, CO2, O3, N2O, CO, NO, NO2, HNO3, CH4		
CIA	CH4-CIA-CH4-0,	0.02-990	CIA due to two CH_4 molecules
	O2-CIA-O2-0,	1150-1950	CIA due to two O_2 molecules
	N2-CIA-N2-0,	0.02-554	CIA due to two N_2 molecules
	N2-CIA-N2-1,	1850-3000	CIA due to two N_2 molecules
	N2-CIA-CH4-0,	0.02-1886	CIA due to N_2 and CH_4 molecule
	CO2-CIA-CO2-0	1-697	CIA due to CO_2 molecules
<i>MT_CKD</i> 1.0	H2O-SelfContCKDMT100,	0-20000	H_2O self continuum
	H2O-ForeignContCKDMT100,	0-20000	H_2O foreign continuum
	O2-CIAfunCKDMT100,	1340-1850	O_2 CIA fundamental band conti.
	O2-v0v0CKDMT100,	7536-8500	O_2 $v0 \leftarrow v0$ band continuum
	O2-v1v0CKDMT100,	9100-11000	O_2 $v0 \leftarrow v1$ band continuum
	N2-CIArotCKDMT100,	0-350	N_2 CIA rotational band continuum
	N2-CIAfunCKDMT100,	2085-2670	N_2 CIA fundamental band conti.
	CO2-CKDMT100	0-10000	CO_2 continuum
MT_CKD 2.5	H2O-SelfContCKDMT250,	0-20000	H_2O self continuum
	H2O-ForeignContCKDMT250,	0-20000	H_2O foreign continuum
	O2-CIAfunCKDMT100,	1340-1850	O_2 CIA fundamental band conti.
	O2-v0v0CKDMT100,	7536-8500	O_2 $v0 \leftarrow v0$ band continuum
	O2-v1v0CKDMT100,	9100-11000	O_2 $v0 \leftarrow v1$ band continuum
	N2-CIArotCKDMT250,	0-350	N_2 CIA rotational band conti.
	N2-CIAfunCKDMT250,	2001-2710	N_2 CIA fundamental continuum
	CO2-CKDMT250	0-10000	CO_2 continuum

CHAPTER 6

Analysis of differences between different continuum models

In this chapter comparison between different continuum models are done, with the help of absorption coefficient and flux calculations.

6.1 Comparison between *MT_CKD*2.5 and *MT_CKD*1.0

For generating Figures 6.1-6.5, line absorption and *MT_CKD* 1.0 species from Table 5.1 for *MT_CKD* 1.0 case and, line absorption and *MT_CKD* 2.5 species for *MT_CKD* 2.5 case are defined as absorption species (abs_species) in ARTS controlfile. That means, total absorption (line + continuum) is considered for generating above mentioned figures.

Figure 6.1 shows continuum absorption coefficient vs wavenumber at the Earth's surface (0 km altitude), for different continuum species of *MT_CKD* 1.0 and *MT_CKD* 2.5. As it can be observed, major changes are in CO_2 continuum, which shows the maximum difference of the order of $10^{-2}m^{-1}$ in the wavenumber range of $2000 - 2500cm^{-1}$. H_2O self continuum shows difference of the order of $10^{-5}m^{-1}$ in the absorption coefficient in the same range as CO_2 shows its maximum difference. While largest difference for H_2O self continuum can be observed in the order of $10^{-3}m^{-1}$ in the wavenumber range of $0 - 500cm^{-1}$. In the same wavenumber region H_2O foreign continuum shows the difference in the order of $10^{-2}m^{-1}$. It is difficult to observe above mentioned difference in Figure 6.1, but it can be clearly observed in magnified plot in Figure 6.2. Figure 6.2 represents same plot as Figure 6.1 in the microwave ($0 - 66.66cm^{-1}$) region. There is no change in O_2 continuum for *MT_CKD* 1.0 to *MT_CKD* 2.5, so only *MT_CKD* 1.0 continuum absorption coefficient of O_2 is plotted.

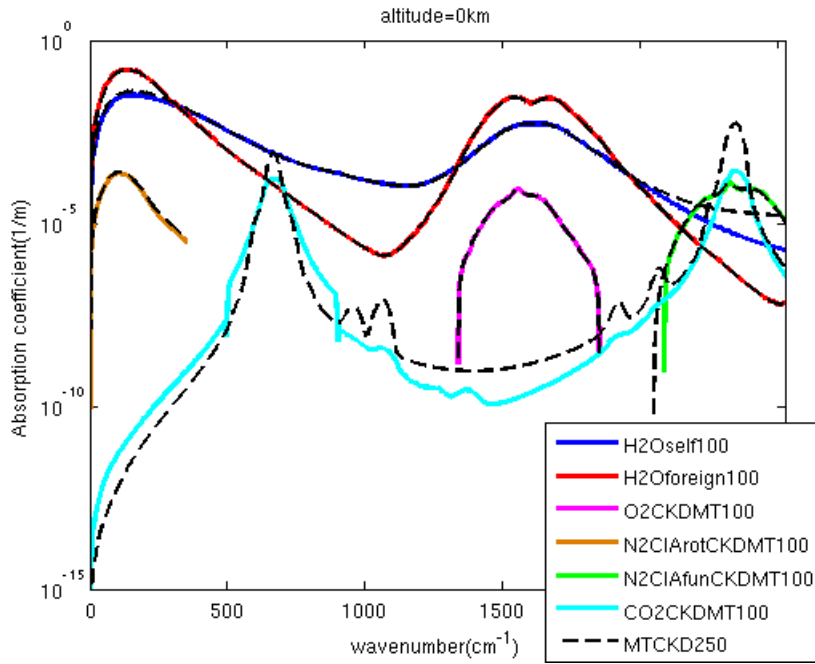


Figure 6.1: Absorption coefficients for *MT_CKD* 2.5 and *MT_CKD* 1.0 vs wavenumber at 0km altitude. In this figure, 'H2Oself100' represents 'H2O-SelfContCKDMT100', 'H2Oforeign100' represents 'H2O-ForeignContCKDMT100', 'O2-MTCKD100' is addition of 'O2-CIAfunCKDMT100', 'O2-v0v0CKDMT100' and 'O2-v1v0CKDMT100', 'CO2CKDMT100' represents 'CO2-CKDMT100' from Table 5.1. Different colors represents different continuum species of *MT_CKD* 1.0, while dashed black lines are for species of *MT_CKD* 2.5. *MT_CKD* 2.5 dashed black lines follows closely *MT_CKD* 1.0 lines of related species.

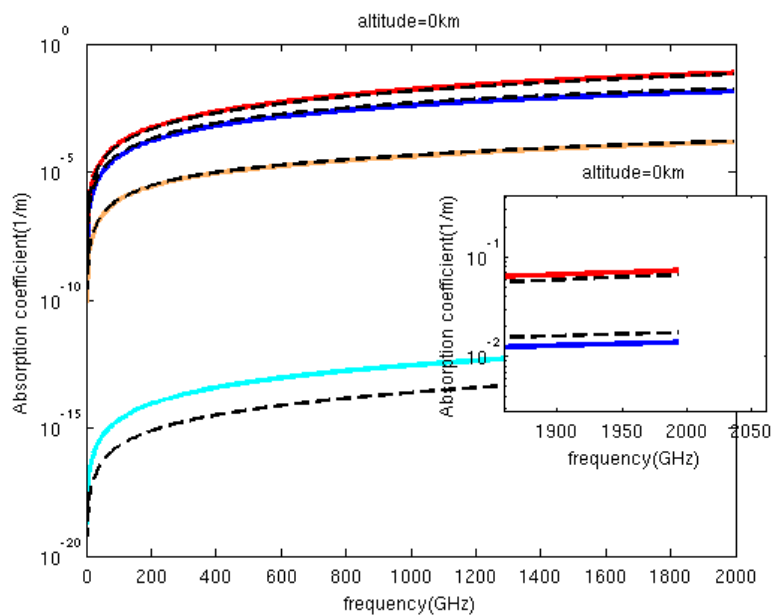


Figure 6.2: Absorption coefficients vs frequency in GHz for *MT_CKD* 2.5 and *MT_CKD* 1.0 at 0km altitude only in microwave range. For explanation of legend see caption of Figure 6.1. Magnified part shows that lines for water vapour self- and foreign continuum does not overlap each other.

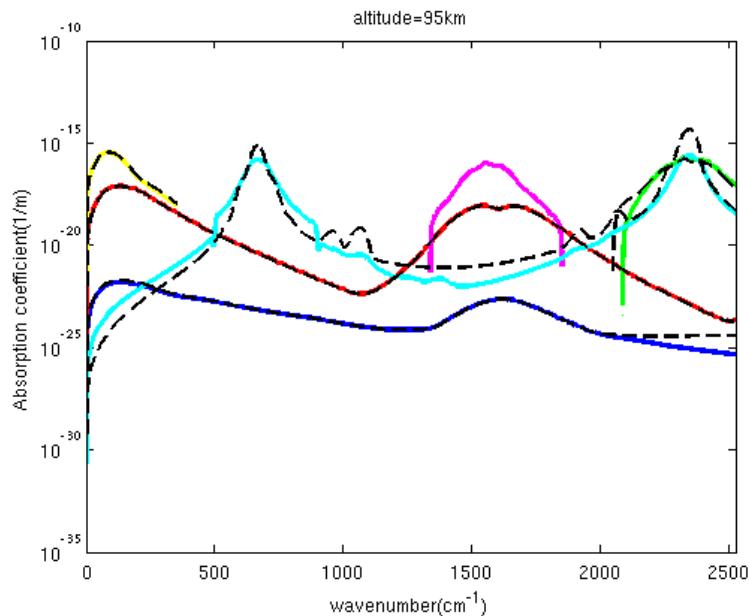


Figure 6.3: Absorption coefficients for *MT_CKD* 2.5 and *MT_CKD* 1.0 at 95km altitude. For explanation of legend see caption of Figure 6.1

In Figure 6.3, absorption coefficients vs wavenumber for different species of *MT_CKD* 1.0 and *MT_CKD* 2.5 are plotted for top of the atmosphere (altitude=95km). Legend of Figure 6.3 is same as Figure 6.1. It can be observed that, at higher altitude contribution of absorption coefficient due to water vapour continuum to the total absorption coefficient decreases. In Figure 6.3 absorption coefficient due to each species is decreased compared to Figure 6.1. We already know that density of the air decreases as we go away from the Earth's surface, which leads to decrease in amount of absorption.

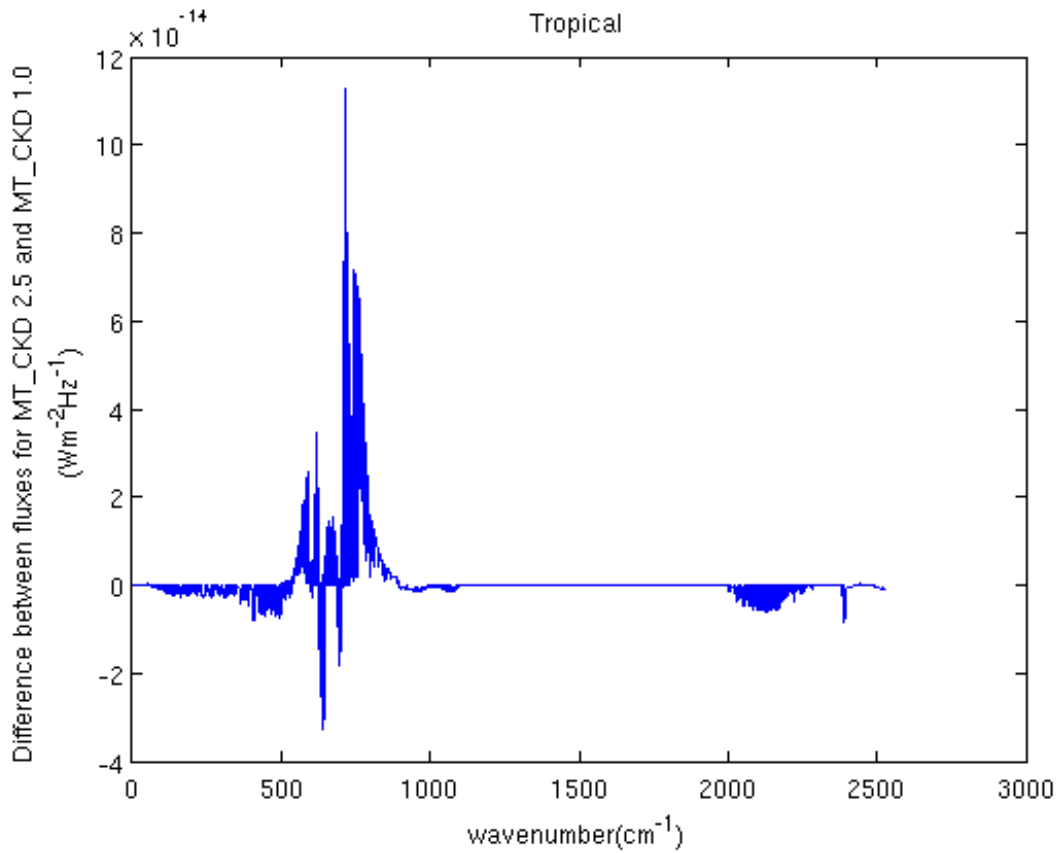


Figure 6.4: Difference between fluxes calculated using *MT_CKD* 2.5 and *MT_CKD* 1.0 vs wavenumber for tropical scenario. For more details see Figure 5.1.

After comparing continuum models considering absorption coefficient, flux comparison is discussed here. To compare the fluxes calculated at the top of atmosphere using both the models, absolute difference and relative difference between the fluxes are plotted against the wavenumber. Absolute difference gives the difference at the specific wavenumber, while relative difference gives the contribution of deviation in the total absorption at the specific wavenumber.

In Figure 6.4 absolute difference between fluxes vs wavenumber calculated using

MT_CKD 2.5 and *MT_CKD* 1.0 is plotted for tropical case. Absolute difference is calculated using Equation 6.1,

$$\Delta F = F_{2.5} - F_{1.0} \quad (6.1)$$

where $F_{2.5}$ and $F_{1.0}$ are fluxes calculated using *MT_CKD* 2.5 and *MT_CKD* 1.0 models respectively. It can be observed that the major difference is found in the wavenumber range of $500 - 1000\text{cm}^{-1}$. Similar kind of behaviour is observed for other atmospheric scenarios as well. From Figure 5.1, it is observed that maximum flux at the top of the atmosphere is lies in wavenumber range of $500 - 1000\text{cm}^{-1}$ (for more details see Figure 1 in Buehler et al. [2005]). So, small change in absorption coefficient (see Figure 6.1) gives large change in flux at the top of the atmosphere in wavenumber range of $500 - 1000\text{cm}^{-1}$. Which continuum species is contributing to major changes in Figure 6.4 is discussed later in the chapter.

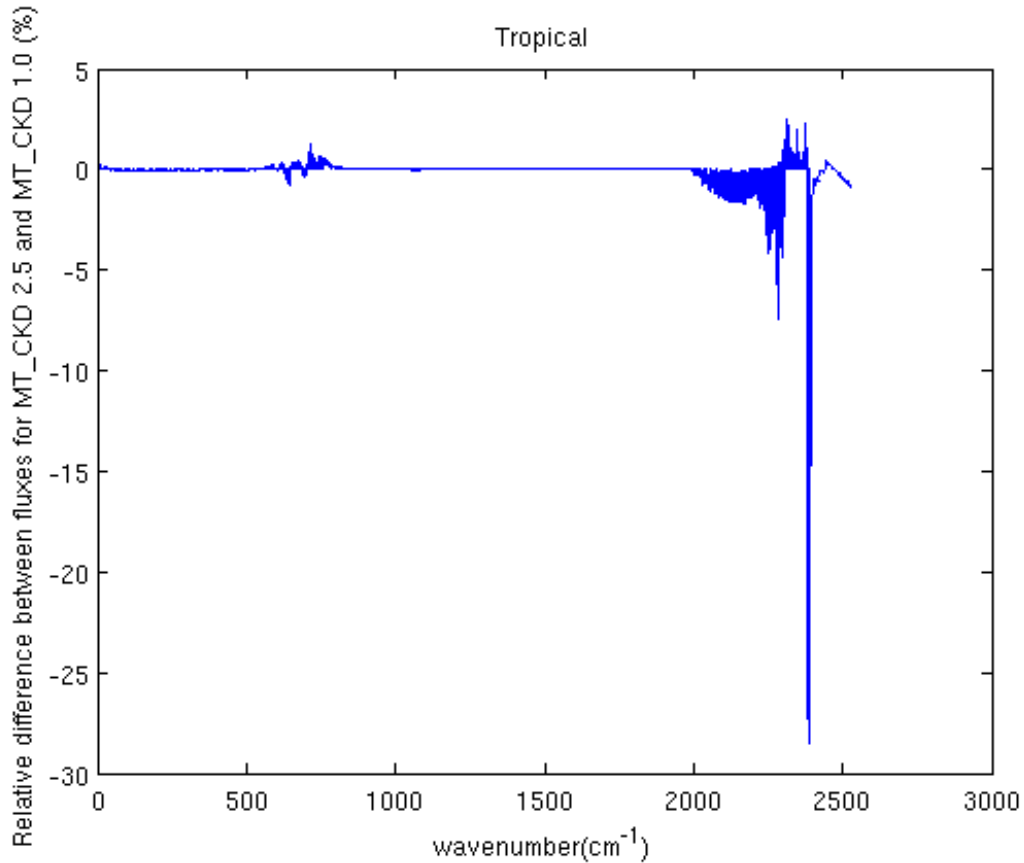
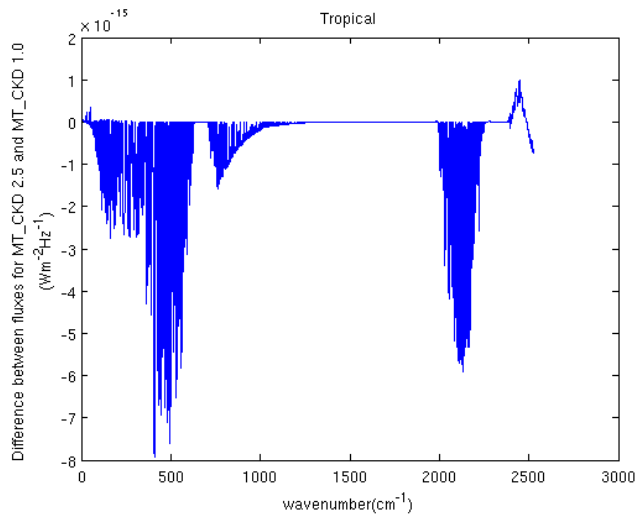


Figure 6.5: Relative difference between fluxes (at the top of the atmosphere) calculated using *MT_CKD* 2.5 and *MT_CKD* 1.0 vs wavenumber. For more details see Figure 5.1.

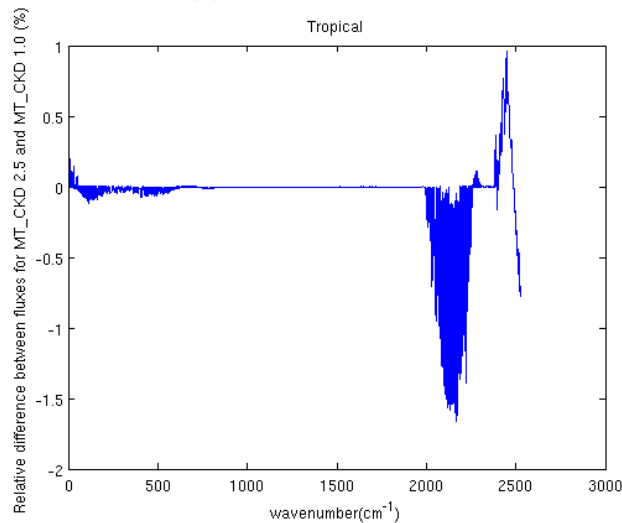
Relative difference is calculated using Equation 6.2, where ΔF is the difference

between fluxes.

$$\% \Delta F = 100 \frac{F_{2.5} - F_{1.0}}{\frac{F_{2.5} + F_{1.0}}{2}} \quad (6.2)$$



(a) Absolute difference



(b) Relative difference

Figure 6.6: Difference between fluxes (at the top of the atmosphere) calculated using *MT_CKD* 2.5 and *MT_CKD* 1.0 without CO_2 continuum. For more details see caption of Figure 5.1.

Relative difference is plotted in Figure 6.5. In Figure 6.5 maximum change of approximately 30% can be observed in the wavenumber range of 2000 – 2500 cm^{-1} .

We checked for other atmospheric scenarios, they show similar kind of behaviour.

To find out which species are contributing most to the absolute and relative difference, we decided to calculate flux differences without CO_2 continuum. For this calculation, all the species from line absorption only and *MT_CKD* 2.5 block are considered except 'CO2-CKDMT250' for *MT_CKD* 2.5 case and, all the species from line absorption only and *MT_CKD* 1.0 block are considered except 'CO2-CKDMT100' for *MT_CKD* 1.0 from Table 5.1. Absolute difference and relative difference in fluxes without CO_2 continuum vs wavenumber is plotted in Figure 6.6. In Figure 6.4 maximum difference in flux can be observed around $11 \times 10^{-14}(\text{Wm}^{-2}\text{Hz}^{-1})$, while in Figure 6.6a maximum difference in flux is approximately $8 \times 10^{-15}(\text{Wm}^{-2}\text{Hz}^{-1})$. In Figure 6.5 maximum relative difference in flux around 30% can be observed, while in Figure 6.6b maximum difference in flux is 1.5%. From this we can say that maximum absolute and relative difference in flux is due to CO_2 continuum.

6.2 Comparison between *MT_CKD*2.5 and *HITRAN_CIA* model

In this section comparison study of *MT_CKD* 2.5 and *HITRAN_CIA* is done. *MT_CKD* 2.5 is the latest version of *MT_CKD* continuum absorption series and *HITRAN_CIA* is recently added to *HITRAN* compilation. Here, for generating Figures 6.7-6.10 line absorption and *MT_CKD* 2.5 species from Table 5.1 for *MT_CKD* 2.5 case and, line absorption and CIA species for *HITRAN_CIA* case is defined as absorption species (abs.species) in ARTS controlfile. That means, total absorption (line + continuum) is considered for generating above mentioned figures.

Figures 6.7 represents absorption coefficient vs wavenumber at Earth's surface (0 km altitude) and Figure 6.8 at the top of the atmosphere (95 km altitude) for different species of *MT_CKD* 2.5 and *HITRAN_CIA* for midlatitude summer case. In Figure 6.7, it can be observed that absorption coefficients for water vapour self- and foreign continuum are having large values compared to others throughout the wavenumber range, while at 95km CO_2 continuum is having larger values than water vapour continuum in most of the wavenumber range, as can be observed in Figure 6.8. *HITRAN_CIA* for CO_2 continuum is having larger value of absorption coefficient in lower wavenumber range than CO_2 continuum for *MT_CKD* 2.5, but after the wavenumber of 500cm^{-1} , absorption coefficient due to 'CO2-CIA-CO2-0' doesn't exist. Absorption coefficient due to N_2 continuum for *MT_CKD* 2.5 and *HITRAN_CIA* overlaps along most of the wavenumber range. Absorption coefficient due to O_2 continuum for *MT_CKD* 2.5 and *HITRAN_CIA* are close to each other, and so is for N_2 continuum. CH_4 is also included in *HITRAN_CIA* model, *HITRAN_CIA* due to $CH_4 - CH_4$ and $N_2 - CH_4$ molecules contributes very little to the total absorption coefficient calculation.

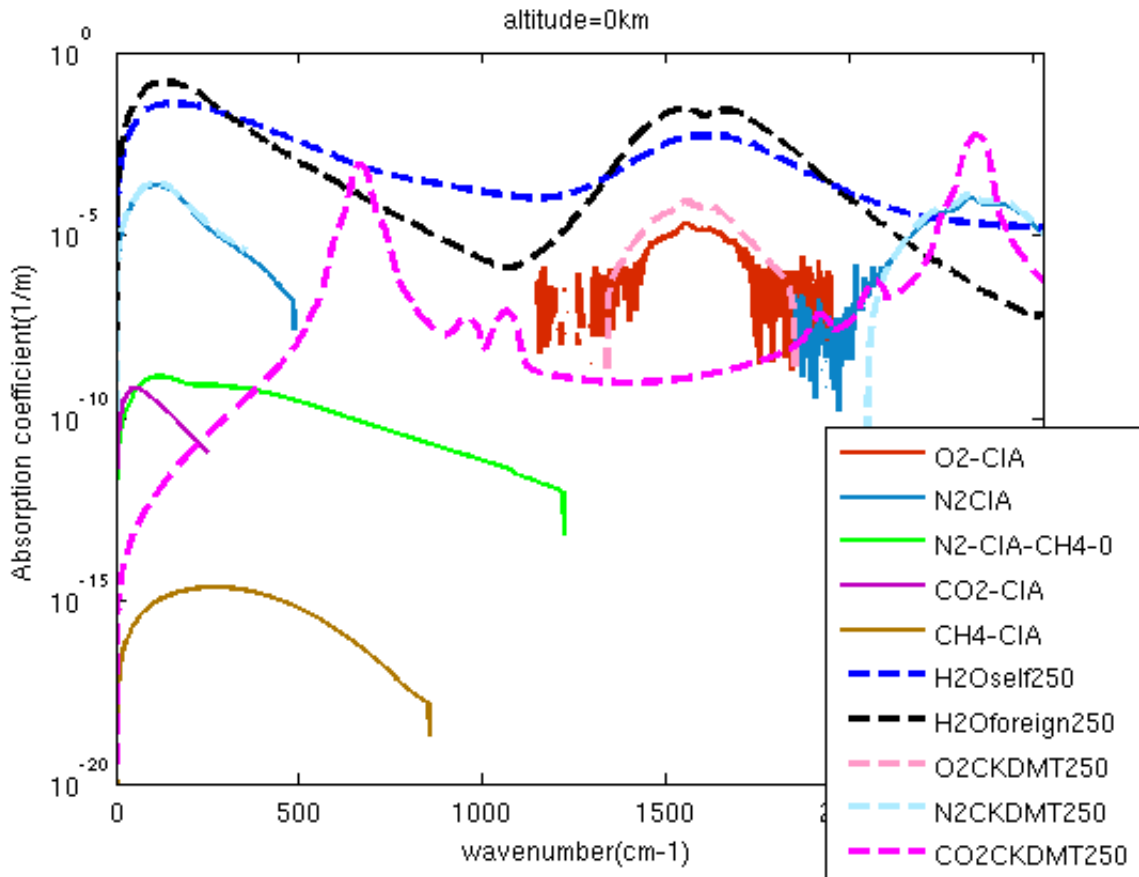


Figure 6.7: Absorption coefficients for *MT_CKD* 2.5 and *HITRAN_CIA* at 0km altitude. Legends 'O2-CIA', 'N2CIA', 'CO2-CIA', 'CH4-CIA', 'H2Oself100', 'H2Oforeign100', 'O2CKDMT250', 'N2CKDMT250', 'CO2CKDMT250' depicts 'O2-CIA-O2-0', 'N2-CIA-N2-0'+ 'N2-CIA-N2-1', 'CO2-CIA-CO2-0', 'CH4-CIA-CH4-0', 'H2O-SelfContCKDMT100', 'H2O-ForeignContCKDMT100', 'O2-CIAfunCKDMT100'+ 'O2-v0v0CKDMT100'+ 'O2v1v0CKDMT', 'N2-CIArotCKDMT100'+ 'N2-CIAfunCKDMT100', 'CO2-CKDMT250' which are explained in Table 5.1

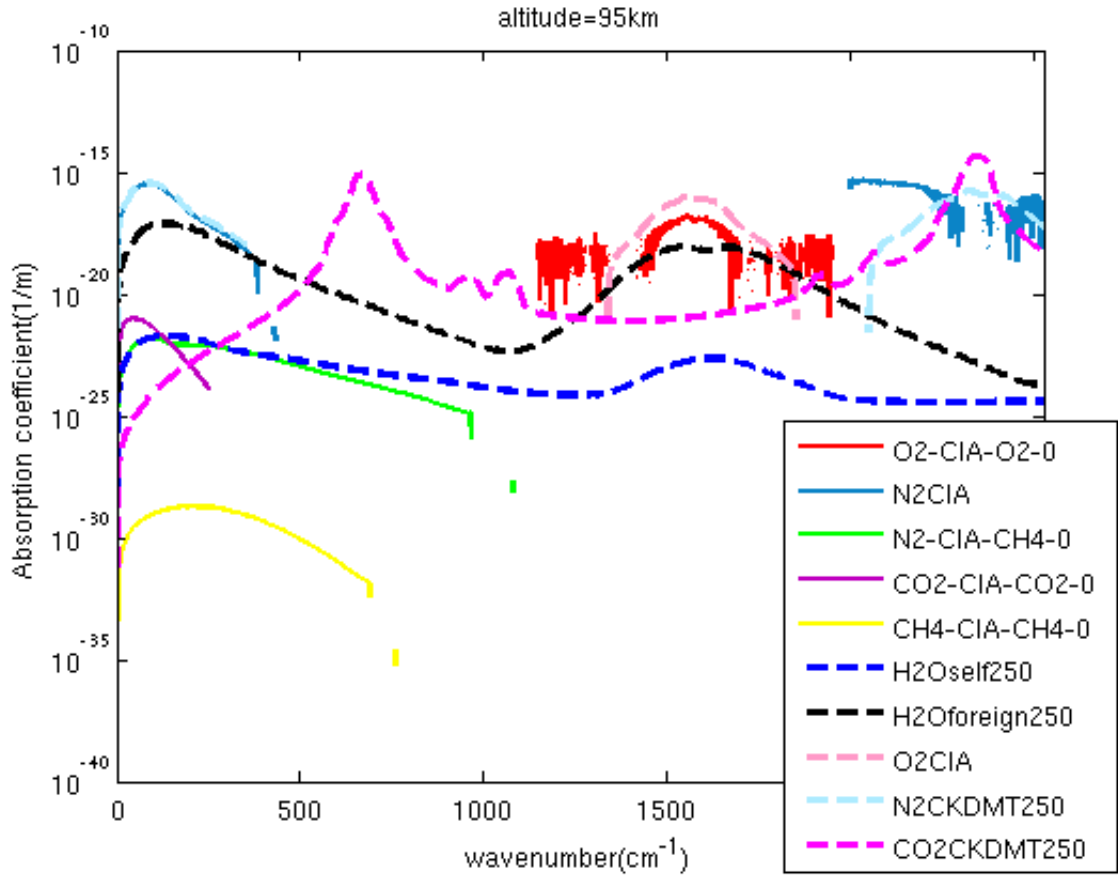


Figure 6.8: Absorption coefficients for *MT_CKD* 2.5 and *HITRAN_CIA* at 95 km altitude. For explanation of legend see caption of Figure 6.7

Below, *MT_CKD* 2.5 and *HITRAN_CIA* is compared considering fluxes. Figure 6.9 shows the absolute difference between flux calculated using above mentioned models. Absolute difference is calculated by replacing $F_{1,0}$ in Equation 6.1 by F_{CIA} . F_{CIA} is flux calculated using *HITRAN_CIA* model at the top of the atmosphere. Here, we can see that large difference is in the wavenumber region of $250 - 1250\text{cm}^{-1}$ and small peak around 1600cm^{-1} . The reason is same as mentioned in section 6.1. Fluxes are having large values in the same wavenumber range, so small difference in absorption coefficient gives large differences in wavenumber range of $250 - 1250\text{cm}^{-1}$.

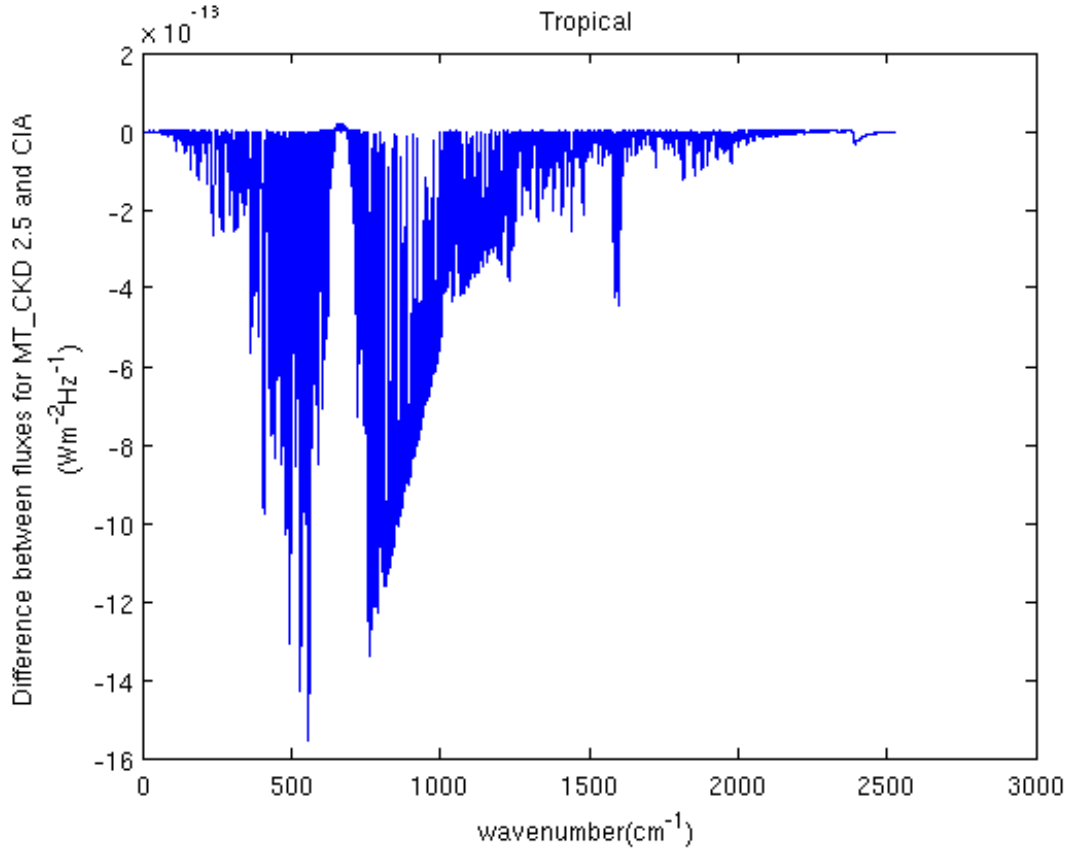


Figure 6.9: Difference between fluxes calculated using *MT_CKD2.5* and CIA vs wavenumber. For more details see caption of Figure 5.1.

In Figure 6.10 relative difference between fluxes calculated using *MT_CKD 2.5* and *HITRAN_CIA* model is plotted against wavenumber. Relative difference is calculated by replacing $F_{1.0}$ in Equation 6.2 by F_{CIA} . It can be observed in Figure 6.10, maximum relative difference lies between 40 – 60%, either in wavenumber range of 1500 – 2000 cm^{-1} or in 2000 – 2500 cm^{-1} .

To find out which species are contributing most in absolute difference between *MT_CKD 2.5* without H_2O continuum and *HITRAN_CIA* are plotted in Figure 6.11 for tropical scenario. From Table 5.1, all species from line absorption and *MT_CKD 2.5* except H_2O continuum species ('H2O-SelfContCKDMT250' and 'H2O-ForeignContCKDMT250') for *MT_CKD 2.5* case and, all species from line absorption and CIA for *HITRAN_CIA* case are considered as absorption species for ARTS calculation. Comparing Figure 6.9 and 6.11, we can say that difference between *MT_CKD 2.5* and *HITRAN_CIA* is majorly coming from H_2O continuum.

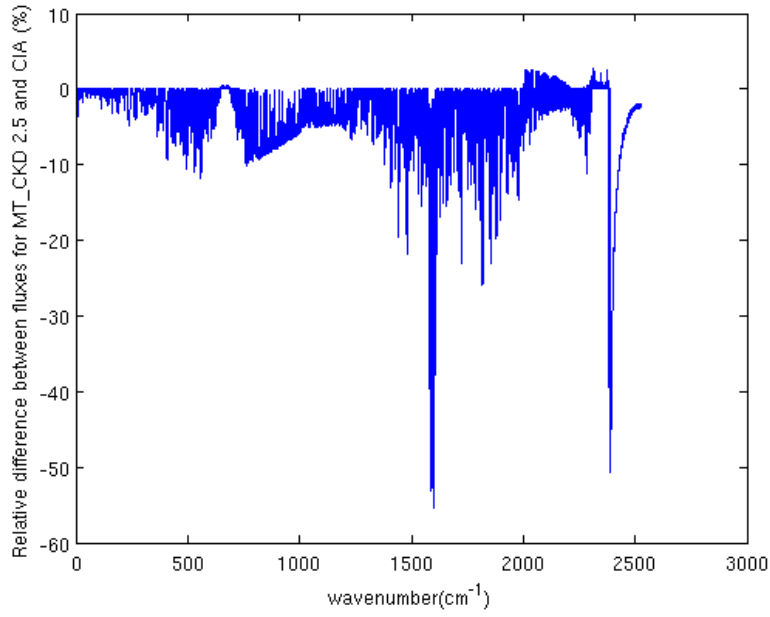


Figure 6.10: Relative difference between fluxes calculated using *MT_CKD* 2.5 and CIA. For more details see caption of Figure 5.1.

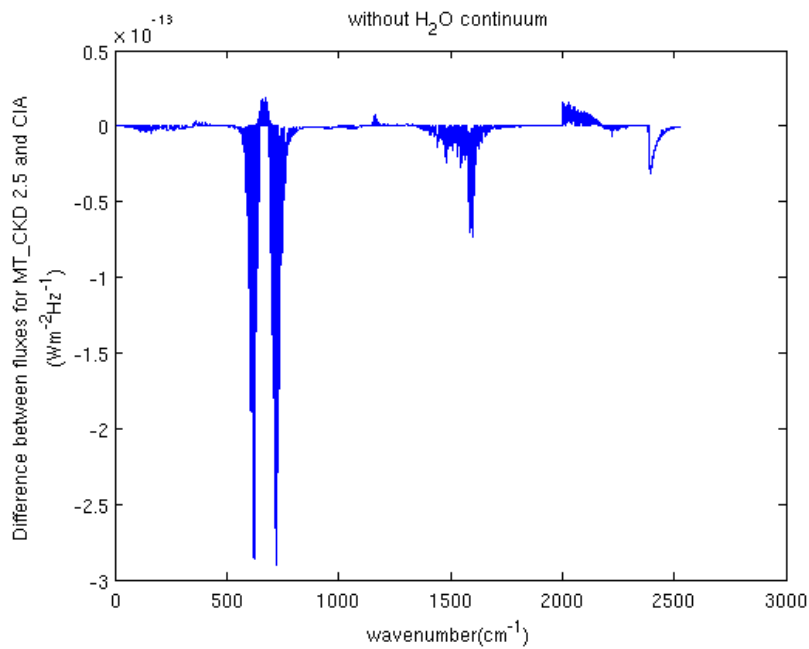


Figure 6.11: Difference between fluxes calculated using *MT_CKD*2.5 and CIA without H_2O continuum. For more details see caption of Figure 5.1

6.3 Comparison between *MT_CKD 2.5*, *MT_CKD 1.0*, *HITRAN_CIA* and line absorption

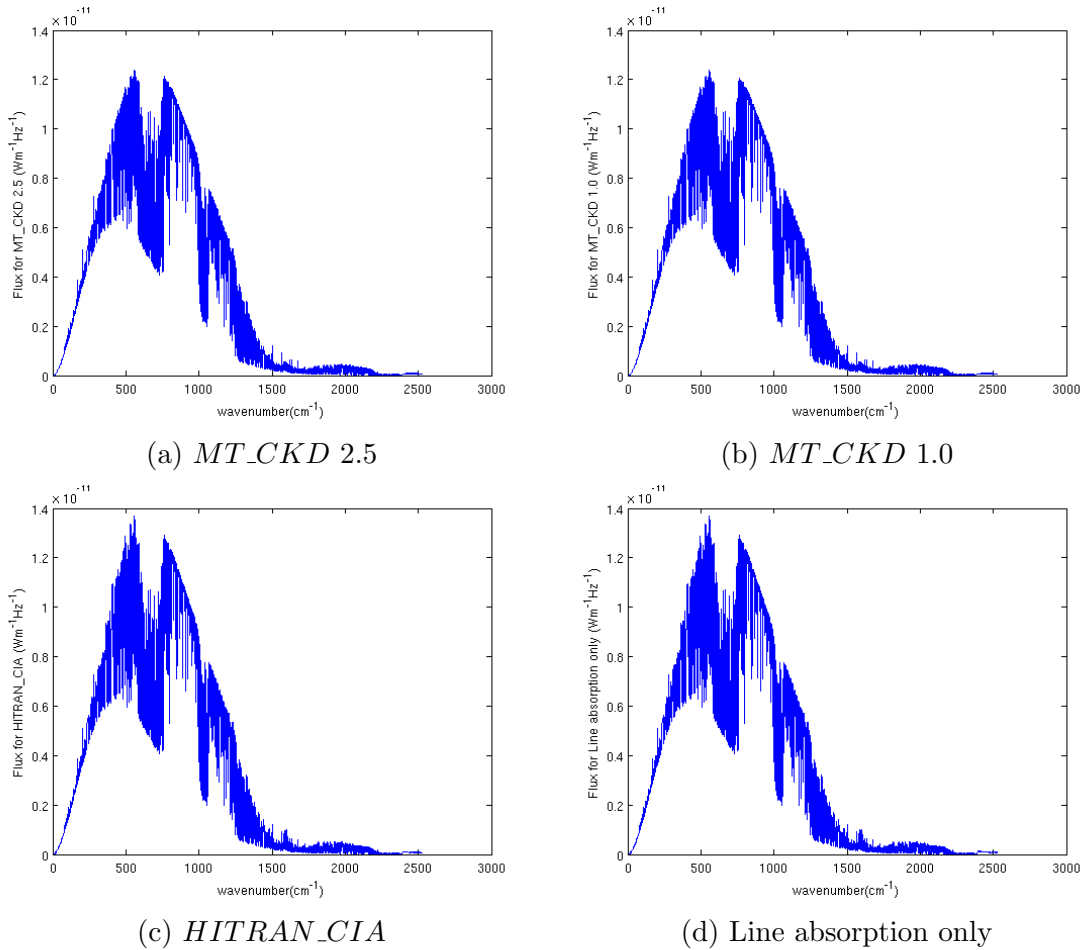


Figure 6.12: Flux vs frequency plots using different methods for midlatitude summer scenario. For more details see caption of Figure 5.1

In this section, we are comparing four different absorption models (*MT_CKD 2.5*, *MT_CKD 1.0*, *HITRAN_CIA* and line absorption) with respect to flux and OLR flux calculation. To find out impact of continuum models on OLR calculation.

Flux calculated using these models are plotted in Figure 6.12. For calculation of flux for *MT_CKD 2.5*, ARTS species mentioned in line absorption and *MT_CKD 2.5* block of Table 5.1 are included in controlfile. For *MT_CKD 1.0*, line absorption and *MT_CKD 1.0*, for *HITRAN_CIA*, line absorption and CIA, for line absorption only line absorption block of Table 5.1 are considered. From this figure we can observe that plots for *MT_CKD 2.5* and *MT_CKD 1.0* are quite similar, while plots for

HITRAN_CIA and line absorption are similar.

It is difficult to retrieve more information from these plots, so we decided to calculate integrated flux (flux integrated over frequency). Integrated flux for different atmospheric scenarios and absorption model is given in Table 6.1. We can see that integrated flux values for *MT_CKD* 2.5 and *MT_CKD* 1.0 are close to each other (difference is of the order of 0.01%), while *HITRAN_CIA* and line absorption have close values (difference is of the order of 0.01%). Difference between *MT_CKD* 2.5 and *HITRAN_CIA* is of the order of 1%. From this we can say that *HITRAN_CIA* lacks many continuum absorption parameters, for example we know that water vapour continuum has not been included in *HITRAN_CIA*. It has also been observed in section 6.2 that water vapour continuum is majorly causes difference in fluxes calculated using *MT_CKD* 2.5 and *HITRAN_CIA*. So, we can predict that water vapour continuum plays important role in OLR.

Values of integrated flux is lesser for continuum models compared to line absorption. Integrated flux is also known as outgoing longwave radiation (OLR) [Buehler et al., 2005]. Here, we can say that, compared to just line absorption, line absorption in addition to continuum, lowers the OLR value. Difference between OLR calculated using *MT_CKD* 2.5 and line absorption is of the order of 1%.

Table 6.1: Integrated Flux

Atmospheric scenarios	<i>MT_CKD</i> 2.5 Integrated flux W/m ²	<i>MT_CKD</i> 1.0 Integrated flux W/m ²	CIA Integrated flux W/m ²	Line absorption only Integrated flux W/m ²
Midlatitude summer(MLS)	270.47	270.37	278.41	278.57
Midlatitude winter(MLW)	222.08	221.98	225.31	225.4190
Subarctic summer(SAS)	254.32	254.22	261.09	261.1937
Subarctic winter(SAW)	192.84	192.75	194.76	194.83
Tropical(T)	276.51	276.43	288.11	288.36

Summary and Conclusions

In this thesis, *MT_CKD* 2.5 continuum model is implemented in ARTS. Implementation was done by understanding the *MT_CKD* 2.5 model FORTRAN code. It was little difficult to implement it, because FORTRAN code gives absorption cross-section as output, while in ARTS we needed absorption coefficient as output for consistency with other continuum models in ARTS. After detail study of *MT_CKD* 2.5 FORTRAN code and *MT_CKD* 1.0 code in ARTS, we found the possibility of implementing it by doing some modifications to the *MT_CKD* 1.0 in ARTS. Modifications are discussed in chapter 4.

Comparison study of *MT_CKD* 2.5, *MT_CKD* 1.0 and *HITRAN_CIA* continuum models (which are incorporated in ARTS) are done during this thesis. For comparison studies, absorption coefficients and fluxes are calculated using ARTS and plotted using matlab, for different atmospheric scenarios in the wavenumber range of $0 - 2525\text{cm}^{-1}$. It should be noted that while computing absorption coefficients and fluxes, line and continuum absorption are considered.

It is observed that largest absolute and relative difference between *MT_CKD* 2.5 and *MT_CKD* 1.0 is due to difference in CO_2 continuum formulation.

It is observed that largest absolute and relative difference between *MT_CKD* 2.5 and *HITRAN_CIA* is coming from water vapour continuum, as *HITRAN_CIA* does not include water vapour continuum.

Comparison of OLR calculated using continuum models *MT_CKD* 2.5, *MT_CKD* 1.0 and *HITRAN_CIA* with line absorption and line absorption are done. It is observed that OLR calculated using *MT_CKD* 2.5 and *MT_CKD* 1.0 shows relative difference of the order of 0.01%, while *MT_CKD* 2.5 and *HITRAN_CIA* shows relative difference of the order of 1%. *HITRAN_CIA* and line absorption shows the relative difference of the order of 0.01%. From this, it can be predicted that OLR values calculated by considering continuum models (in addition to the line absorption model) decreases, especially absorption due to water vapour continuum.

Relative difference between OLR calculated using *MT_CKD* 2.5 and *MT_CKD* 1.0 is not very large, but relative difference between fluxes (for these models) can be as

high as 30% in some frequency ranges. It can be source of inaccuracy for instruments which use those frequency ranges.

From the above discussion and studies conducted in this thesis, it can also be conclude that replacing *MT_CKD* 2.5 or *MT_CKD* 1.0 with *HITRAN_CIA* for OLR calculation might give large error, because it does not include water vapour continuum.

Bibliography

- Gail P Anderson, SA Clough, FX Kneizys, JH Chetwynd, and E Po Shettle. Afl atmospheric constituent profiles (0.120 km). Technical report, DTIC Document, 1986.
- Hartmut H Aumann, Moustafa T Chahine, Catherine Gautier, Mitchell D Goldberg, Eugenia Kalnay, Larry M McMillin, Hank Revercomb, Philip W Rosenkranz, William L Smith, David H Staelin, et al. Airs/amsu/hsb on the aqua mission: Design, science objectives, data products, and processing systems. *Geoscience and Remote Sensing, IEEE Transactions on*, 41(2):253–264, 2003.
- Di Cecca S Griffin MK Schwartz SD Bicknell, WE and A Flusberg. Search for lowabsorption regions in the 1.6 and 2.1 μm atmospheric windows. *Journal of Directed Energy*, 2:151–161, 2006.
- J Boissoles, C Boulet, RH Tipping, Alex Brown, and Q Ma. Theoretical calculation of the translation-rotation collision-induced absorption in $n_2 - n_2$, $o_2 - o_2$, and $n_2 - o_2$ pairs. *Journal of Quantitative Spectroscopy and Radiative Transfer*, 82(1):505–516, 2003.
- Aleksandra Borysow and Lothar Frommhold. Collision-induced rototranslational absorption spectra of $n_2 - n_2$ pairs for temperatures from 50 to 300 k. *The Astrophysical Journal*, 311:1043–1057, 1986.
- SA Buehler, Patrick Eriksson, T Kuhn, A Von Engeln, and C Verdes. Arts, the atmospheric radiative transfer simulator. *Journal of Quantitative Spectroscopy and Radiative Transfer*, 91(1):65–93, 2005.
- SA Buehler, A von Engeln, E Brocard, VO John, T Kuhn, and Patrick Eriksson. Recent developments in the line-by-line modeling of outgoing longwave radiation. *Journal of Quantitative Spectroscopy and Radiative Transfer*, 98(3):446–457, 2006.
- Darrell E Burch and Robert L Alt. Continuum absorption by h₂o in the 700-1200 cm^{-1} and 2400-280 cm^{-1} windows. *Continuum absorption by H₂O in the 700-1200 cm^{-1} and 2400-280 cm^{-1} windows AFGL*, 1, 1984.
- SA Clough, FX Kneizys, and RW Davies. Line shape and the water vapor continuum. *Atmospheric research*, 23(3):229–241, 1989.

- SA Clough, MW Shephard, EJ Mlawer, JS Delamere, MJ Iacono, K Cady-Pereira, S Boukabara, and PD Brown. Atmospheric radiative transfer modeling: a summary of the aer codes. *Journal of Quantitative Spectroscopy and Radiative Transfer*, 91(2):233–244, 2005.
- Shepard A Clough, Michael J Iacono, and Jean-Luc Moncet. Line-by-line calculations of atmospheric fluxes and cooling rates: Application to water vapor. *Journal of Geophysical Research: Atmospheres (1984–2012)*, 97(D14):15761–15785, 1992.
- JS Delamere, SA Clough, VH Payne, EJ Mlawer, DD Turner, and RR Gamache. A far-infrared radiative closure study in the arctic: Application to water vapor. *Journal of Geophysical Research: Atmospheres (1984–2012)*, 115(D17), 2010.
- SA Clough EJ Mlawer, DC Tobin. *mt_ckd 2.5*. [http : //rtweb.aer.com/continuum_frame.html](http://rtweb.aer.com/continuum_frame.html).
- Walter M Elsasser. Mean absorption and equivalent absorption coefficient of a band spectrum. *Physical Review*, 54(2):126, 1938.
- Eric L Fleming, Sushil Chandra, JJ Barnett, and M Corney. Zonal mean temperature, pressure, zonal wind and geopotential height as functions of latitude. *Advances in Space Research*, 10(12):11–59, 1990.
- Lothar Frommhold. *Collision-induced absorption in gases*, volume 2. Cambridge University Press, 2006.
- Lothar Frommhold, III Collisional Induction, and Virial Expansions. Collision-induced spectroscopy. *Encyclopedia of physical science and technology*, 3:166, 1987.
- Stephen F Fulghum and Michael M Tilleman. Interferometric calorimeter for the measurement of water-vapor absorption. *JOSA B*, 8(12):2401–2413, 1991.
- Yung YL Goody RM. *Atmospheric Radiation: theoretical basis*, volume 61. Oxford University Press, 1989.
- RO Knuteson, HE Revercomb, FA Best, NC Ciganovich, RG Dedecker, TP Dirx, SC Ellington, WF Feltz, RK Garcia, HB Howell, et al. Atmospheric emitted radiance interferometer. part i: Instrument design. *Journal of Atmospheric and Oceanic Technology*, 21(12):1763–1776, 2004.
- Walter J Lafferty, Alexander M Solodov, Alfons Weber, Wm Bruce Olson, and Jean-Michel Hartmann. Infrared collision-induced absorption by n_2 near $4.3 \mu\text{m}$ for atmospheric applications: measurements and empirical modeling. *Applied optics*, 35(30):5911–5917, 1996.
- J Lamouroux, H Tran, AL Laraia, RR Gamache, LS Rothman, IE Gordon, and J-M Hartmann. Updated database plus software for line-mixing in CO_2 infrared spectra

- and their test using laboratory spectra in the 1.5 – 2.3 μm region. *Journal of Quantitative Spectroscopy and Radiative Transfer*, 111(15):2321–2331, 2010.
- B Maté, C Lugez, Gerald T Fraser, and Walter J Lafferty. Absolute intensities for the o_2 1.27 μm continuum absorption. *Journal of Geophysical Research: Atmospheres (1984–2012)*, 104(D23):30585–30590, 1999.
- Eli J Mlawer, Shepard A Clough, Patrick D Brown, Thomas M Stephen, Joseph C Landry, Aaron Goldman, and Frank J Murcray. Observed atmospheric collision-induced absorption in near-infrared oxygen bands. *Journal of Geophysical Research: Atmospheres (1984–2012)*, 103(D4):3859–3863, 1998.
- Eli J Mlawer, Vivienne H Payne, Jean-Luc Moncet, Jennifer S Delamere, Matthew J Alvarado, and David C Tobin. Development and recent evaluation of the *mt_ckd* model of continuum absorption. *Philosophical Transactions of the Royal Society A: Mathematical, Physical and Engineering Sciences*, 370(1968):2520–2556, 2012.
- C Emde T R Sreerekha-C Melsheimer P Eriksson, S A Buehler and O Lemke. *ARTS–2 User Guide*. ARTS Development Team, 2011. regularly updated versions available at <http://www.sat.ltu.se/arts/docs/>.
- Vivienne H Payne, Eli J Mlawer, Karen E Cady-Pereira, and J Moncet. Water vapor continuum absorption in the microwave. *Geoscience and Remote Sensing, IEEE Transactions on*, 49(6):2194–2208, 2011.
- HM Pickett, RL Poynter, EA Cohen, ML Delitsky, JC Pearson, and HSP Müller. Submillimeter, millimeter, and microwave spectral line catalog. *Journal of Quantitative Spectroscopy and Radiative Transfer*, 60(5):883–890, 1998.
- C Richard, IE Gordon, LS Rothman, M Abel, L Frommhold, Magnus Gustafsson, J-M Hartmann, C Hermans, WJ Lafferty, GS Orton, et al. New section of the hitran database: Collision-induced absorption (cia). *Journal of Quantitative Spectroscopy and Radiative Transfer*, 113(11):1276–1285, 2012.
- WL Ridgway, RA Moose, and AC Cogley. Atmospheric transmittance/radiance computer code fascod2. Technical report, DTIC Document, 1982.
- CP Rinsland, R Zander, JS Namkung, CB Farmer, and RH Norton. Stratospheric infrared continuum absorptions observed by the atmos instrument. *Journal of Geophysical Research: Atmospheres (1984–2012)*, 94(D13):16303–16322, 1989.
- CP Rinsland, JS Levine, A Goldman, ND Sze, MKW Ko, and DW Johnson. Infrared measurements of hf and hcl total column abundances above kitt peak, 1977–1990: Seasonal cycles, long-term increases, and comparisons with model calculations. *Journal of Geophysical Research: Atmospheres (1984–2012)*, 96(D8):15523–15540, 1991.

- Philip W Rosenkranz. *Absorption of microwaves by atmospheric gases*. John Wiley and Sons, 1993.
- Philip W Rosenkranz. Water vapor microwave continuum absorption: A comparison of measurements and models. *Radio Science*, 33(4):919–928, 1998.
- LS Rothman, IE Gordon, Y Babikov, A Barbe, D Chris Benner, PF Bernath, Manfred Birk, L Bizzocchi, V Boudon, LR Brown, et al. The hitran2012 molecular spectroscopic database. *Journal of Quantitative Spectroscopy and Radiative Transfer*, 130:4–50, 2013.
- Murry L Salby. *Fundamentals of atmospheric physics*, volume 61. Academic press, 1996.
- HJP Smith, DJ Dube, ME Gardner, SA Clough, and FX Kneizys. Fascode-fast atmospheric signature code (spectral transmittance and radiance). Technical report, DTIC Document, 1978.
- S Solomon, RW Portmann, RW Sanders, and JS Daniel. Absorption of solar radiation by water vapor, oxygen, and related collision pairs in the earth’s atmosphere. *Journal of Geophysical Research: Atmospheres (1984–2012)*, 103(D4):3847–3858, 1998.
- Doucen RL Rosenmann L Hartmann J-M Boulet C Thibault F, Moreau G. Infrared collision-induced absorption by o_2 near 6 : 4 mm for atmospheric applications: measurements and empirical modeling. *Applied Optics*, 36:563–567, 1997.
- JH Van Vleck and VF Weisskopf. On the shape of collision-broadened lines. *Reviews of Modern Physics*, 17(2-3):227–236, 1945.